

Doctorate Dissertation (Censored)

博士論文 (要約)

Elucidation of mechanism regulating gene expression profiles via an interaction between a virus sensor, LGP2, and an RNA silencing enhancer, TRBP

( ウイルスセンサーLGP2 が RNA サイレンシング促進因子 TRBP と相互作用して遺伝子発現を制御する機構の解明 )

A Dissertation Submitted for Degree of Doctor of Philosophy

December 2018

平成 30 年 12 月博士 (理学) 申請

Department of Biological Sciences, Graduate School of Science,

The University of Tokyo

東京大学大学院理学系研究科

生物科学専攻

Yuko Nakano

中野 悠子

## **Abstract**

In mammalian cells, the antiviral response is induced by introduction of exogenous double-stranded RNAs (dsRNAs) including viral RNAs. On the other hand, RNA silencing is induced by endogenous microRNAs (miRNAs), which function as a post-transcriptional gene regulation system. Both pathways are triggered by dsRNAs in the cytoplasm. However, since any factor which functions in both pathways had not identified, it was remained unknown whether there is a crosstalk between these pathways. The aim of this study is to reveal the crosstalk and its molecular mechanism in mammalian cells.

I found that a virus sensor protein, laboratory of genetics and physiology 2 (LGP2), interacts with an RNA silencing enhancer, TAR-RNA binding protein (TRBP). I revealed that TRBP has a binding preference for a specific type of miRNAs whose stem region has tight base-pairing, and LGP2 regulates the expression of specific genes by repressing RNA silencing mediated by TRBP-bound miRNAs. Furthermore, I elucidated that TRBP-bound miRNAs repress the expression of genes related to apoptosis directly and indirectly via transcription factors in the condition without viral infection. However, in the condition mimicking virus infection. Accordingly, these findings indicated that LGP2-TRBP interaction functions as a defense system against viral infection by regulating apoptotic cell death of virus-infected cells.

# Contents

<b>Abbreviation</b>	1
<b>1. Introduction</b>	4
<b>1.1. Gene silencing mediated by small non-coding RNAs</b>	4
<b>1.2. Antiviral response</b>	5
1.2.1. RLRs family and TLR3	6
1.2.2. Substrates of RLRs and TLR3	7
1.2.3. Proposed function of LGP2 in RLR signaling	8
<b>1.3. TRBP</b>	9
1.3.1. Identification	9
1.3.2. Gene characterization	9
1.3.3. Domain structure	9
1.3.4. The function of TRBP on RNA silencing	10
<b>1.4. Antiviral response and RNA silencing</b>	10
<b>2. The effect of virus sensor, LGP2, on RNA silencing via the interaction with an RNA silencing enhancer, TRBP</b>	11
<b>2.1. Introduction</b>	11
<b>2.2. Materials and Methods</b>	11
2.2.1. Cell culture	11
2.2.2. Small interfering RNA (siRNA)	11
2.2.3. Plasmid construction	12
2.2.4. Generation of doxycycline-inducible FLAG-tagged TRBP expression cell line	13
2.2.5. Immunoprecipitation assay	13
2.2.6. Western blotting	13
2.2.7. Establishment of knock-out cells using CRISPR/Cas9 system	14
2.2.8. T7E1 assay	14
2.2.9. Dual-luciferase assay for measuring RNA silencing activity	15

2.2.10.	RT-PCR	15
2.2.11.	RNA immunoprecipitation (RIP)-sequencing (seq) analysis	16
<b>2.3.</b>	<b>Results</b>	17
2.3.1.	Interaction between a virus sensor, LGP2, and an RNA silencing enhancer, TRBP	17
2.3.2.	The effects of RLRs on RNA silencing activity in HeLa cells	18
2.3.3.	Identification of TRBP-bound pre-miRNAs by RIP-sequencing analysis	22
2.3.4.	Secondary structural features of TRBP-bound pre-miRNAs	23
2.3.5.	The effect of LGP2 on maturation of TRBP-bound pre-miRNAs	24
2.3.6.	The effect of LGP2 on target mRNA levels of mature miRNA biosynthesized from TRBP-bound pre-miRNAs	25
<b>2.4.</b>	<b>Discussion</b>	25
<b>3.</b>	<b>Elucidation of gene network regulated by TRBP during virus infection</b>	27
<b>3.1.</b>	<b>Introduction</b>	27
<b>3.2.</b>	<b>Materials and Methods</b>	27
3.2.1.	Cell culture	27
3.2.2.	qRT-PCR	27
3.2.3.	Plasmid construction	28
3.2.4.	Immunoprecipitation assay	28
3.2.5.	Western blotting	29
3.2.6.	Preparation of RNA-sequencing library	29
3.2.7.	RNA-sequencing analysis	30
<b>3.3.</b>	<b>Results</b>	31
3.3.1.	The effect of poly(I:C) transfection on HeLa cells	31
3.3.2.	Interaction between virus sensors RLRs and an RNA silencing enhancer TRBP in poly(I:C)-transfected HeLa cells	32
3.3.3.	The effect of transfected poly(I:C) on RNA silencing activity	33
3.3.4.	Identification of upregulated genes by poly(I:C) transfection in both WT and TRBP <sup>-/-</sup> HeLa cells	34

3.3.5.	Identification of miRNAs downregulated through LGP2-TRBP interaction by poly(I:C) transfection	35
3.3.6.	Gene Ontology analysis of the predicted target genes of the downregulated mature miRNAs in WT cells but not in TRBP <sup>-/-</sup> cells	35
3.4.	Discussion	37
4.	Conclusion	42
	Acknowledgement	44
	References	45
	Figures and Tables	46

## Abbreviation

aa	amino acid
AGO	Argonaute
bp	base pair
bpp	base-pairing probability
CARD	caspase activation and recruitment domains
Cardif	CARD adaptor inducing IFN- $\beta$
CDKN	Cyclin-dependent kinase inhibitor
cDNA	complementary DNA
CRISPR	clustered regularly interspaced short palindromic repeat
CTD	C-terminal domain
DAVID	Database for Annotation, Visualization and Integrated Discovery
DGCR8	DiGeorge syndrome critical region gene 8
DNA	deoxyribonucleic acid
dsRBD	dsRNA-binding domain
dsDNA	double-stranded DNA
dsRNA	double-stranded RNA
DUF	domain of unknown function
ECD	ectodomain
GO	Gene Ontology
HEK	human embryonic kidney
HIV-1	human immunodeficiency virus type 1
IAV	Influenza virus
IFIH1	interferon induced with helicase C domain 1
IFN	interferon

ISG	IFN-stimulated gene
JEV	Japanese encephalitis virus
LGP2	laboratory of genetics and physiology 2
LRR	leucine-rich repeat
MAVS	mitochondrial antiviral signaling protein
MDA5	melanoma differentiation-associated gene 5
NDV	Newcastle disease virus
NLRs	NOD-like receptors
NOD	nucleotide-binding oligomerization domain
nt	nucleotide
OAS	2'-, 5'-oligoadenylate synthetase
PAGE	SDS-polyacrylamide gel electrophoresis
PAZ	piwi-argonaute-zwille
PCR	polymerase chain reaction
PEI	polyethyleneimine
poly(I:C)	polyinosinic-polycytidylic acid
qRT-PCR	quantitative RT-PCR
RIG-I	retinoic acid-inducible gene I
RIP-seq	RNA immunoprecipitation sequencing
RISC	RNA-induced silencing complex
RLC	RISC-loading complex
RLRs	RIG-I-like receptors
RNA	ribonucleic acid
RNase	ribonuclease
RPM	reads per million mapped reads
rRNA	ribosomal RNA
RT-PCR	real-time PCR

SeV	Sendai virus
SDS	sodium dodecyl sulfate
SDS-PAGE	SDS polyacrylamide gel electrophoresis
sgRNA	single guide RNA
siRNA	small interfering RNA
ssRNA	single-stranded RNA
TAR	trans-activation-responsive
TBS	Tris buffered saline
TLR	Toll-like receptor
TRAF	TNA receptor-associated factor
TRIF	TIR-domain-containing adaptor-inducing interferon- $\beta$
TRBP	TAR-RNA binding protein
T7EI	T7 endonuclease I
VISA	virus-induced signaling adaptor
VPg	viral protein linked to the genome
VSV	Vesicular stomatitis virus
WT	wild type



# 1. Introduction

## 1.1. Gene silencing mediated by small non-coding RNAs

MicroRNAs (miRNAs) are a class of small non-coding RNAs found in almost eukaryotes and play a critical role in post-transcriptional regulation of gene expression. In human, approximately 2,000 miRNAs have been registered on the miRNA database, miRBase (Griffiths-Jones *et al.*, 2006). Many studies have highlighted the importance of miRNAs in various biological processes, including cell proliferation, differentiation, embryonic development, and oncogenesis (Bartel *et al.*, 2004, Croce *et al.*, 2009).

Primary transcripts of miRNAs (pri-miRNAs) of > 1 kb long are transcribed from genome by RNA polymerase II (Lee *et al.*, 2004) (Figure 1). The pri-miRNAs are processed into stem-loop structured intermediates, termed precursor miRNAs (pre-miRNAs), of approximately 70-nucleotide (nt) with 2-nt overhang at 3' end by the microprocessor complex consisting of the nuclear RNase III Drosha and a cofactor DiGeorge syndrome critical region gene 8 (DGCR8) (Lee *et al.*, 2003). In the processing procedure, Drosha interacts with the junction between double-stranded RNA (dsRNA) and single-stranded RNA (ssRNA) of pri-miRNA stem and the UG-motif at the basal junction. Drosha measures and cleaves at the ~11 bp from the junction. On the other hand, DGCR8 interacts with the apical stem and the UGU-motif at the apical loop using two dsRNA-binding domains (dsRBDs), and enhances RNA-binding ability of Drosha (Nguyen *et al.*, 2015, Kwon *et al.*, 2016). The processed pre-miRNAs are exported from the nucleus to the cytoplasm by a transport complex, comprising Exportin-5 (XPO5), GTP-binding nuclear protein RAN, and GTP (Yi *et al.*, 2003, Bohnsack *et al.*, 2004). In the cytoplasm, the pre-miRNAs are further processed into approximately 22-nt miRNA duplexes with 2-nt overhang at 3' end by a complex consisting of RNase III Dicer and TAR RNA-binding protein (TRBP). In the processing procedure, TRBP binds to pre-

miRNAs via its dsRBDs to facilitate the cleavage by Dicer (Provost *et al.*, 2002, Chendrimada *et al.*, 2005). TRBP interacts with stem region of dsRNA and locates 3'-end of dsRNA onto Dicer, where the PAZ domain verifies 3'-overhang (Fareh *et al.*, 2016). TRBP releases dsRNA lacking 2-nt 3'-overhang, whereas TRBP transfer dsRNA harboring 2-nt 3'-overhang to Dicer. The miRNA duplex is loaded onto Argonaute (AGO) in the RNA-induced silencing complex (RISC)-loading complex (RLC) (Chendrimada *et al.*, 2005, MacRae *et al.*, 2008). The miRNA duplex is unwound within AGO and one strand of them, termed a guide strand, is loaded onto AGO proteins to form RISC and functions as a guide to target mRNA (MacRae *et al.*, 2008, Wang *et al.*, 2009, Maniataki *et al.*, 2005). The guide strand recognizes target mRNA by base-pairing complementarity. The target recognition is dominated by miRNA binding to 3' UTR of target mRNA essentially through the 7-nt sequence at 2-8 nt from 5' end, which is referred to as "seed" (Grimson *et al.*, 2007). Upon target recognition, RISC leads to mRNA destabilization or translational repression and represses expression of the target genes. Human AGO family consists of AGO1-4 (Doi *et al.*, 2003) and only AGO2 has cleavage activity of target mRNA (Liu *et al.*, 2004). All AGOs contribute to miRNA-mediated gene silencing (Su *et al.*, 2009). Target mRNA sequences are recognized by essentially 7-nt long seed sequence of miRNA, which results in that one miRNA is capable of targeting and repressing multiple genes simultaneously (Bartel *et al.*, 2004, Grimson *et al.*, 2007, Lim *et al.*, 2005).

## **1.2. Antiviral response**

In mammals, virus infection induces the innate immune response as a viral immediate defense system. In this system, the intracellular or extracellular molecular signature known as pathogen-associated molecular patterns (PAMPs) are detected by the host pattern recognition receptors (PRRs), and its downstream signaling induces the production of interferons (IFNs) and inflammatory cytokines to establish an intracellular antiviral state. Viral RNAs are detected by Toll-like receptor 3 (TLR3) in the endosome (Nishiya *et al.*, 2004) or Retinoic

acid-inducible gene I (RIG-I)-like receptors (RLRs) in the cytoplasm (Yoneyama *et al.*, 2004) (Figure 2).

#### 1.2.1. RLRs family and TLR3

RLRs consist of RIG-I (also known as DDX58), melanoma differentiation-associated gene 5 (MDA5) (also known as interferon induced with helicase C domain 1, IFIH1), and laboratory of genetics and physiology 2 (LGP2) (also known as DHX58). All of three RLRs are members of DExD/H-box RNA helicase family. They express at low level in virus non-infected cells, whereas they are rapidly induced via secreted IFN upon virus infection. They share similar domain structure of ATPase/Helicase domain and a C-terminal domain (CTD) (Figure3). ATPase/Helicase domain is necessary for RNA binding, ATP hydrolysis, and conformational change (Kowalinski *et al.*, 2011, Beckham *et al.*, 2013). The CTD is responsible for detection of specific RNA substrate features (Cui *et al.*, 2008). RIG-I and MDA5 have a two N-terminal caspase activation and recruitment domains (CARDs), respectively, but LGPs does not have CARD. The CARDs are essential for downstream signaling (Yoneyama *et al.*, 2005). RIG-I and MDA5 bind to CARD of adaptor protein IFN- $\beta$  promoter stimulator protein 1 (IPS-1) (also known as MAVS; mitochondrial antiviral signaling protein, Cardif; CARD adaptor inducing IFN- $\beta$ , and VISA; virus-induced signaling adaptor) via their CARDs. RIG-I and MDA5 form the inactive (closed) conformation, in which the CARDs and CTD interact with ATPase/Helicase domain resulting in the masking CARDs, in the virus non-infected cells. Upon binding viral RNA to RIG-I and MDA5, the CARDs are exposed by a conformational change that leads to downstream signaling by the interaction between their CARDs and the CARD of IPS-1. Once RIG-I and MDA5 binds to IPS-1, oligomerization of IPS-1 is facilitated. The oligomerization is essential for recruitment and activation of TBK1, and I $\kappa$ B kinases (IKKs) via TNF receptor-

associated factors (TRAFs; TRAF2, TRAF3, and TRAF6) resulting in the phosphorylation of transcriptional factors, IRF3 and IRF7 (Saha *et al.*, 2006, Fang *et al.*, 2017). The phosphorylated IRF3 and IRF7 induce type I interferon (IFN) that leads to the production of IFN-stimulated genes (ISGs) (Sadler *et al.*, 2008). On the other hand, LGP2 lacking N-terminal CARDs has been thought to be incapable of such signal transduction. Thus, the functional machinery of LGP2 remained unknown, but it is considered that LGP2 functions through essentially different machinery from RIG-I or MDA5.

TLR3 is a member of type I transmembrane proteins TLR family and localized in the endosomal membrane (Nishiya *et al.*, 2004). TLR3 detects viral dsRNA and transduces signaling by interacting with an adaptor protein TIR-domain-containing adaptor-inducing interferon- $\beta$  (TRIF) (Nishiya *et al.*, 2004). TRIF leads to an activation of NF $\kappa$ B and MAPKs and the induction of inflammatory cytokines by interacting with TRAF6, and a phosphorylation of IRF3 and type I IFN induction by interacting with TRAF3 (Sato *et al.*, 2003, Doyle *et al.*, 2002).

### **1.2.2. Substrates of RLRs and TLR3**

RIG-I detects 5'-triphosphorylated or 5'-diphosphorylated blunt end of dsRNA of some types of viruses, such as paramyxoviruses including influenza virus (IAV), Japanese encephalitis virus (JEV), Newcastle disease virus (NDV), Sendai virus (SeV), and vesicular stomatitis virus (VSV), as non-self RNA (Hornung *et al.*, 2006, Goubau *et al.*, 2014). Such RNA substrates have been considered to be derived from various origins, e.g., virus replication intermediates, viral transcripts, or virus genomes from negative strand RNA viruses or self-RNA cleaved by RNaseL (Rehwinkel *et al.*, 2010, Schlee *et al.*, 2009, Malathi *et al.*, 2007). In other words, self-RNAs without a 5'-triphosphate are not recognized as PAMPs by RIG-I, for example, mRNA containing the 5'-terminal 7-methyl-guanosins (5' m7G) cap

structure or transfer RNA and ribosomal RNA (rRNA) trimmed at their 5'-end by exonuclease. On the other hand, MDA5 binds to the internal region of dsRNAs without 5'-end preference. It is suggested that MDA5 sensed viral RNA which is protected by the viral protein linked to the genome (VPg) attached to 5'-end and not detected by RIG-I, such as picornavirus including encephalomyocarditis virus (EMCV) and Theiler's murine encephalitis virus (TMEV) (Pathak *et al.*, 2002). Furthermore, RIG-I detects short dsRNA up to 1 kbp, at least longer than 19 bp (Schlee *et al.*, 2009, Marq *et al.*, 2011), and MDA5 detects long dsRNA more than 1 kbp (Kato *et al.*, 2008). Contrary to RIG-I and MDA5, the specific feature of substrates of LGP2 has not been well-described. TLR3 has N-terminal ectodomain (ECD), which consists of 22 leucine-rich repeats (LRRs). TLR3 binds to viral dsRNA longer than 40 bp as a substrate via its ECD (Liu *et al.*, 2008).

### **1.2.3. Proposed function of LGP2 in RLR signaling**

Although LGP2 binds to dsRNA much stronger than RIG-I and MDA5 (the affinity to dsRNA; LGP2 >> RIG-I > MDA5), only LGP2 does not have CARD which is necessary for downstream signaling (Yoneyama *et al.*, 2005). LGP2 interacts with both RIG-I and MDA5 (Saito *et al.*, 2007). Therefore, LGP2 is thought to be unable to transduce signal by itself but regulate the signaling via interaction with RIG-I or MDA5. However, the function of LGP2 on RLR signaling has not been clear yet due to various reports advocating both positive and negative function for antiviral response by LGP2. Deficient of LGP2 repressed the production of type I IFN by RIG-I and MDA5 during various viral infection, indicating that LGP2 positively regulates RIG-I and MDA5 signaling (Satoh *et al.*, 2010, Suthar *et al.*, 2012). On the other hand, overexpression of LGP2 negatively regulate IRF-3 and NF- $\kappa$ B induced by SeV infection (Rothenfusser *et al.*, 2005).

### 1.3. TRBP

#### 1.3.1. Identification

TRBP was identified as a factor interacting with the human immunodeficiency virus type 1 (HIV-1) trans-activation-responsive (TAR) RNA (Gatignol *et al.*, 1991). HIV-1 gene expression is activated by HIV-1 Tat protein via an association with TAR RNA. The TAR RNA sequence is located in the R region of the long terminal repeat (LTR) (Hauber *et al.*, 1988), which is folded into a stem-bulge-loop structure. TRBP activates HIV-1 gene expression by binding to TAR RNA synergistically with Tat.

#### 1.3.2. Gene characterization

Human TRBP is encoded on *tarbp2* gene located on chromosome 12 and one pseudogene is located on chromosome 3 (Duarte *et al.*, 2000). The *tarbp2* gene has two promoter regions and generates two isoforms, TRBP1 and TRBP2 (Bannwarth *et al.*, 2001). The two isoforms have different 5' end of the mRNAs resulting in 21 additional amino acids for TRBP2 compared to TRBP1. Both TRBP1 and TRBP2 activate the HIV-1 expression.

#### 1.3.3. Domain structure

TRBP has three dsRBDs, which adopt a common  $\alpha$ - $\beta$ - $\beta$ - $\beta$ - $\alpha$  fold (Figure 3). Two N-terminal dsRBDs (dsRBD1 and dsRBD2) are canonical type A dsRBDs and the C-terminal dsRBD (dsRBD3) is a non-canonical type B dsRBD. Type A dsRBD harbors three RNA-binding regions (St Johnston *et al.*, 1992). All of the regions are conserved in dsRBD1 and dsRBD2 of TRBP but dsRBD3 lacks two of them (Gleghorn *et al.*, 2014). Especially two lysine residues at 80 and 81 in dsRBD1 and those at 210 and 211 in dsRBD2 are essential for binding to dsRNA (Takahashi *et al.*, 2013). Thus, it is considered that TRBP binds dsRNA with the N-terminal dsRBD1 and dsRBD2, and the C-terminal dsRBD3 mediates protein-protein interaction.

#### **1.3.4. The function of TRBP on RNA silencing**

TRBP was identified as an enhancer of RNA silencing (Chendrimada *et al.*, 2005, Haase *et al.*, 2005). In RNA silencing, since pre-miRNAs are processed by Dicer to generate mature miRNAs in the cytoplasm, Dicer is considered to be essential for miRNA biogenesis. TRBP locates in the cytoplasm and interacts with Dicer independently of RNA via its dsRBD3 (Daniels *et al.*, 2009, Haase *et al.*, 2005). The TRBP-binding site in Dicer is a 165 amino acid (aa) region located from 267 aa to 431 aa between the ATPase and the helicase motifs (Daniels *et al.*, 2009) (Figure 3). TRBP shows much higher RNA-binding affinity than Dicer and promotes Dicer processing by greatly increasing the RNA-binding affinity of Dicer (Chendrimada *et al.*, 2005, Chakravarthy *et al.*, 2010). In addition, TRBP is considered to enhance the accuracy of the sites of Dicer cleavage (Wilson *et al.*, 2015, Kim *et al.*, 2014). Furthermore, TRBP-Dicer complex associates with dsRNA to form a ternary complex with AGO, thus TRBP is considered to enhance the loading of miRNA onto AGO.

#### **1.4. Antiviral response and RNA silencing**

In mammalian cells, both the antiviral response and RNA silencing are triggered by dsRNA in the cytoplasm (Figure 2). However, since any interrelation between these two pathways has not been demonstrated, and has been considered as independent pathways. Previous report demonstrated that an unknown factor regulates RNA silencing by interacting with an RNA silencing enhancer, TRBP (Takahashi *et al.*, 2014). Therefore, the two pathways are considered to be linked via the unknown factor. The aim of this study is to reveal the crosstalk via the unknown factor and its molecular mechanism in mammalian cells.

## **2. The effect of virus sensor, LGP2, on RNA silencing via the interaction with an RNA silencing enhancer, TRBP**

### **2.1. Introduction**

During virus infection, viral RNAs are sensed by RLRs in the cytoplasm and trigger antiviral response with the production of IFN. On the other hand, endogenous small non-coding RNAs, miRNAs, regulate expression of multiple genes with various dsRNA-binding proteins (dsRBPs) in RNA silencing. Both antiviral response and RNA silencing are triggered by dsRNAs in the cytoplasm. Hence, an interrelationship between both pathways were expected. However, a factor regulating both pathways has not been found and the two pathways are considered to be independent pathways.

### **2.2. Materials and Methods**

#### **2.2.1. Cell culture**

Human HEK293 cells and HeLa wild type (WT) cells, TRBP<sup>-/-</sup> cells, LGP2<sup>-/-</sup> cells, and RIG-I<sup>-/-</sup> cells were cultured in Dulbecco's Modified Eagle's Medium (Wako) with 10% Fetal Bovine Serum (Gibco) at 37°C with 5% CO<sub>2</sub>.

#### **2.2.2. Small interfering RNA (siRNA)**

The siRNAs used for gene knockdown experiments were chemically synthesized (Sigma-Adrich, Shanghai GenePharma). The sequences of siRNA are shown in Table 1.



### 2.2.3. Plasmid construction

The N-terminal FLAG-tagged TRBP (FLAG-TRBP) was amplified from TRBP-Myc expression plasmid by PCR with primers containing the restriction enzyme sites of NheI or HindIII at either end. The amplified fragment was digested with NheI and HindIII and cloned into pcDNA5 vector (Invitrogen) digested with the same restriction enzymes. The expression plasmids of pre-miRNA like RNA targeting firefly luciferase, pre-miLuc (pSilencer-FL774) was constructed as described previously (Ui-Tei *et al.*, 2004). Plasmids encoding the LGP2 or its deletion mutants (WT,  $\Delta$ CTD, and CTD) were kindly provided from Dr. Fujita (Narita *et al.*, 2014). Full length TRBP was cloned into pcDNA5-FRT-TO-FLAG/HA-SBP-B (Okada-Katsumata *et al.*, 2012) digested with NheI and HindIII (pcDNA5-TRBP-WT).

Single guide RNA (sgRNA) against LGP2 was designed using CRISPRdirect (Naito *et al.*, 2015, <https://crispr.dbcls.jp>) targeting exon 1 of the genomic LGP2 gene (Figure 6). TRBP has two transcriptional variants, TRBP1 and TRBP2. sgRNA against TRBP was designed targeting exon 2 of the genomic TRBP gene, which is included in both variants (Figure 7). sgRNA against RIG-I was designed targeting exon 1 of the genomic RIG-I gene (Figure 11). The oligonucleotide sequences shown in Table 2 were digested with *Bbs*I and cloned into the pSuperCRISPR vector (Ui-Tei *et al.*, 2017).

For the construction of a plasmid expressing miR-106b, named Tough Decoy (TuD)-miR-106b, oligonucleotide pairs were annealed and cloned into the pmU6-TuD-shuttle digested with *Bsm*BI. pmU6-TuD-shuttle was kindly provided from Drs. Iba and Haraguchi (Haraguchi *et al.*, 2009). The sequences of oligonucleotides used were shown in Table 3.

#### **2.2.4. Generation of doxycycline-inducible FLAG-tagged TRBP expression cell line**

Flp-In T-REX 293 host cell line was purchased from Life Technologies. pcDNA5-TRBP-WT expressing N-terminal FLAG-tagged TRBP (1 µg) was co-transfected with 1 µg of pOG44 Flp-Recombinase Expression Vector (Life Technologies) into the Flp-In T-REX 293 host cell line using 6 µg of polyethyleneimine (PEI). Selection of successfully transfected cells of pcDNA5-TRBP-WT was performed with 100 µg / mL hygromycin 48 hours after the transfection. The expression of FLAG-TRBP protein was confirmed by western blot with anti-FLAG antibody.

#### **2.2.5. Immunoprecipitation assay**

One day before transfection, WT HeLa cells were plated at  $1.2 \times 10^6$  cells / dish in a 6 cm dish. The cells were transfected with a plasmid encoding FLAG-TRBP using PEI and harvested a day later using Trypsin-EDTA (Wako). The cells were washed with  $1 \times$  PBS and lysed in lysis buffer (10 mM Hepes-NaOH [pH 7.9], 1.5 mM  $MgCl_2$ , 10 mM KCl, 0.5 mM DTT, 140 mM NaCl, 1 mM EDTA, 1 mM  $Na_3VO_4$ , 10 mM NaF, 0.5% NP-40 and complete protease inhibitor). The cell lysates were mixed with 30 µL of Protein G Sepharose 4B (Sigma) and rotated at 4°C for 2 hours with 2.5 µg of mouse anti-FLAG antibody (Sigma). The beads were washed twice with wash buffer containing 300 mM NaCl and once with lysis buffer. To elute the bound proteins,  $2 \times$  SDS-PAGE sample buffer (30 µL) was added and the beads were boiled for 5 min. RLRs and Dicer were separated using 10 % polyacrylamide gel and TRBP was separated using 12.5 % polyacrylamide gel, and detected by western blotting.

#### **2.2.6. Western blotting**

Cells were treated with IFN and lysed 24 hours later using 100 µL of  $1 \times$  passive lysis buffer (PLB) (Promega). Proteins were separated by SDS-polyacrylamide gel electrophoresis (PAGE) and electrophoretically transferred on polyvinylidene

fluoride membranes by the Trans-Blot Turbo Transfer System (Bio-Rad). The membranes were treated with the blocking buffer, TBS-Tween (TBS-T; 20 mM Tris-HCl [pH 7.5], 150 mM NaCl, 0.1% Tween 20) with 5% Difco skim milk (Becton, Dickinson and Company) for 1 hour, and incubated with specific antibodies in Can Get Signal immunoreaction enhancer solution (TOYOBO) at 4°C overnight. The membranes were washed in TBS-T for 10 minutes three times and reacted with HRP-linked anti-rabbit or anti-mouse antibody (GE Healthcare) at room temperature for 1 hour. The membranes were washed in TBS-T for 10 minutes three times, incubated with ECL Prime Western Blotting Detection Reagent (GE Healthcare), and analyzed using the ImageQuant LAS4000 (GE Healthcare).

#### **2.2.7. Establishment of knock-out cells using CRISPR/Cas9 system**

One day before a transfection, HeLa cells were plated at  $6 \times 10^5$  cells / well in 6-well plate. Cells were transfected with 2 µg of the pSUPER-CRISPR guide TTTA and 2 µg of a plasmid encoding the Cas9 protein using Lipofectamine 2000 (Invitrogen). 30 hours after transfection, puromycin at 2 µg / mL was added and selected for 2 days. Mutation on genome was detected by T7EI (T7 endonuclease I) assay and limiting dilution of cells was performed twice for isolation of knock-out cells. To confirm the successful knock-out of each gene, sequencing of genomic DNA and western blotting were performed. The sequences of primers used for sequencing are shown in Table 2.

#### **2.2.8. T7EI assay**

Cells plated in one well of 96-well plate were treated with 96.7 µL of genomic DNA extraction buffer (50 mM Tris-HCl [pH 8.0], 1 mM EDTA [pH 8.0], 1 % Tween-20), added with 3.3 µL of proteinase K and 0.025 µL of RNase A, and incubated at 55 °C overnight. Then cell lysate was incubated at 95 °C for 30 min to inactivate proteinase

K and genomic DNA was extracted. Next, the DNA fragment containing sgRNA target site was amplified using the genomic DNA as a template by PCR. The PCR products were reannealed after thermal denaturation, and were incubated with 3.3  $\mu$ L of 10  $\times$  NEBuffer 2 (New England Biolabs), following the treatment with 0.5  $\mu$ L T7EI at 37 °C for 30 min. The fragments were separated by 6 % nondenaturing polyacrylamide gel electrophoresis. The used primers were shown in Table 2.

#### **2.2.9. Dual-luciferase assay for measuring RNA silencing activity**

RNA silencing activity was measured by luciferase reporter assay. One day before a transfection, the knock-out HeLa cells of TRBP, RIG-I, or LGP2, or the knocked down HeLa cells by specific siRNA against TRBP, RIG-I, or LGP2 were plated at 1  $\times$  10<sup>5</sup> cells / well in 24-well plate with or without IFN treatment. Cells were transfected with 0.5  $\mu$ g of pGL3-Control vector (Promega) encoding firefly *luciferase* and pSilencer-3.1-H1-puro vector encoding pre-miRNA against firefly *luciferase* (pre-miLuc) using Lipofectamine 2000 (Invitrogen). pRL-SV40 vector 0.1  $\mu$ g (Promega) encoding *Renilla luciferase* was co-transfected as an internal control. Twenty-four hours after transfection, cells were lysed with 100  $\mu$ L of 1  $\times$  PLB (Promega). Luciferase activities were detected by Dual-Luciferase Reporter Assay System (Promega), and Relative luciferase activity (firefly luciferase activity)/(Renilla luciferase activity) was calculated.

#### **2.2.10. RT-PCR**

One day before transfection, WT or LGP2<sup>-/-</sup> HeLa cells were plated at 2  $\times$  10<sup>5</sup> cells / well in a well of 12-well plate. The cells were transfected with a plasmid encoding miRNA inhibitor (TuD-miR-106b) at 1  $\mu$ g / well using Lipofectamine 2000 and harvested them 24 hours after the transfection. Total RNAs were extracted from the cells using FastGene RNA Premium (Nippon Genetics). The cDNA of total RNAs

were synthesized with random primer using High Capacity cDNA Reverse Transcription Kits (Applied Biosystems). The cDNAs of mature miR-106b and miR-19b were synthesized with each miRNA specific RT-primer. mRNA levels of IFN- $\beta$  and 2'-, 5'-oligoadenylate synthetases (OASs) (OAS1, OAS2, and OAS3) were measured by qRT-PCR using the cDNA as a template. As a control, mRNA level of tubulin was measured. The mature miRNA levels were detected by RT-PCR using the cDNA of each miRNA as a template and separated in 2 % agarose gel electrophoresis. The signal intensity was determined using Image J. The primer used are shown in Table 4.

#### **2.2.11. RNA immunoprecipitation (RIP)-sequencing (seq) analysis**

Flp-In 293 TRBP cells was plated into a 9-cm dish with 1  $\mu$ g / mL doxycycline and immunoprecipitated by anti-FLAG antibody. Extracted RNAs were measured by Qubit2.0 Fluorometer (Life Technologies) and the qualities were confirmed by Bioanalyzer (Agilent). rRNA was removed by Ribo-Zero rRNA Removal kit (AR BROWN). RNA-seq was carried out using cDNA libraries prepared from small RNA fraction (15-110 nt) by illumina Truseq small RNA kit and sequenced 36 nt by HiSeq 2500 in single-end mode.

Thirty-six nt reads were extracted as pre-miRNAs using cutadapt (version 1.11, Marcel *et al.*, 2012). Since I confirmed that the quality score of all reads were enough high using FastQC (version 0.11.5) (Andrews *et al.*, 2010), filtering based on the quality score was not performed. All of the 36 nt reads were mapped to the reference sequence (RefSeq) database (GRCh38) using Bowtie (version 1.1.2) allowing for 2 nt mismatches and annotated according to the miRNA database (miRBase release 21, Kozomara *et al.*, 2014). After counting raw reads using HTSeq (Anders *et al.*, 2015), reads corresponding to pre-miRNAs were normalized by RPM (reads per million mapped reads). Enrichment rate was calculated by the following

formula:  $(IP_{RPM} + 1)/(input_{RPM} + 1)$ . Base-pairing probability of each pre-miRNA was calculated by CentroidFold with default parameters (Sato *et al.*, 2008) using pre-miRNA sequences. In miRBase, pre-miRNAs are registered with additional sequences at the 5'- or 3'-end of actual pre-miRNA sequence. Then pre-miRNA sequences were prepared by cleaving off the additional sequence at the 5'- or 3'- end, based on registered mature miRNA sequence. The pre-miRNAs whose sequence reads were zero in input RNAs or immunoprecipitated RNAs were excluded for the calculation of sequence read enrichment by immunoprecipitation.

RNA extraction was performed by F. Murakami and RNA-seq was performed by Suzuki-lab.

## **2.3. Results**

### **2.3.1. Interaction between a virus sensor, LGP2, and an RNA silencing enhancer, TRBP**

TRBP is an important factor involved in RNA silencing. TRBP binds to pre-miRNAs, and recruits Dicer to promote processing of pre-miRNA. However, previous study suggested that an unidentified factor other than Dicer interacts with TRBP and regulates RNA silencing activity (Takahashi *et al.*, 2014). Takahashi et al. reported that TRBP has much lower affinity to siRNA with a double-stranded DNA (dsDNA) seed than that with dsRNA seed. However, knockdown analysis of TRBP revealed that TRBP enhances RNA interference activity triggered by siRNA with a dsDNA seed at the same level as siRNA with dsRNA seed, suggesting that a novel regulates the recruitment of TRBP to siRNA. TRBP interacts with Dicer via its ATPase/Helicase domain (Daniels *et al.*, 2009). Thus, the candidate of novel interacting factor was searched by BLASTP search using amino acid sequence of helicase domain of Dicer. The result revealed that RLRs, especially LGP2, were similar to Dicer (Figure 3) with low expect (*E*) values, which is a parameter that

describes the number of hits one can expect to see by chance when searching a database. Among RLRs, LGP2 showed the lowest *E*-value. To examine whether RLRs can also interact with TRBP, a plasmid encoding N-terminal FLAG-tagged TRBP (FLAG-TRBP) was transfected into HeLa cells in the presence or absence of interferon (IFN), which induces the expression of RLRs. Then, immunoprecipitation was performed using anti-FLAG antibody and each endogenous RLR was detected by western blotting using anti-LGP2, anti-RIG-I, and anti-MDA5 antibodies, respectively. The protein levels of all RLRs were increased by IFN treatment, whereas that of Dicer, an RNA silencing factor, was not changed (Figure 4). Dicer was immunoprecipitated with TRBP in the presence or absence of IFN, but not with GFP (Figure 5). Among RLRs, LGP2 was immunoprecipitated with TRBP in HeLa cells with or without IFN treatment, but the amounts of immunoprecipitated LGP2 protein increased after IFN treatment. However, almost no RIG-I and MDA5 were immunoprecipitated with TRBP even in the IFN-treated HeLa cells.

### **2.3.2. The effects of RLRs on RNA silencing activity in HeLa cells**

LGP2 interacted with an RNA silencing enhancer, TRBP, shown in Figure 5, suggesting that LGP2 may be involved in the regulation of RNA silencing. To investigate the effect of LGP2 on RNA silencing activity through the interaction with TRBP, LGP2 knock-out (LGP2<sup>-/-</sup>) and TRBP knock-out (TRBP<sup>-/-</sup>) HeLa cells were generated using clustered regularly interspaced short palindromic repeat (CRISPR)/Cas9 genome editing method. First, to generate LGP2<sup>-/-</sup> HeLa cells, sgRNA was designed against exon 1 of *lgp2* gene using CRISPRdirect (Naito *et al.*, 2015) (Figure 6A). 4 days after the transfection of a plasmid encoding the sgRNA into HeLa cells (Figure 6A), the mutation efficiency on the genome was measured by T7EI assay. The result showed that approximately 17.4 % of the genomic region of *lgp2* was mutated in the cells transfected (Figure 6B). Then the cells were isolated by

two rounds of limiting dilution to obtain clonal cells derived from a cell with *lgp2* mutation. I confirmed mutations in *lgp2* region by sequencing (Figure 6C). Furthermore, I ascertained disappearance of LGP2 protein by western blotting (Figure 6D). Next, to generate TRBP<sup>-/-</sup> HeLa cells, sgRNA was designed against exon 2 of *tarbp2* gene in the same procedure with the generation of LGP2<sup>-/-</sup> HeLa cells (Figure 7A). TRBP has two transcriptional variants and the exon2 is a common region of them. The plasmid expressing sgRNA against TRBP was transfected into HeLa cells and the mutation efficiency on the genome was approximately 11 % by T7EI assay (Figure 7B), and clonal cells were isolated by two rounds of limiting dilution. I confirmed mutations in *tarbp2* region by sequencing and disappearance of TRBP protein by western blotting (Figure 7C, D).

RNA silencing activity was measured by dual-luciferase reporter assay. WT HeLa cells were treated with or without IFN and transfected with plasmids encoding firefly *luciferase* and pre-miLuc. A plasmid encoding *Renilla luciferase* was simultaneously transfected as an internal control and each luciferase luminescent activity was measured. The pre-miLuc against firefly *luciferase* was considered to repress the relative luciferase activity (firefly luciferase luminescent / *Renilla luciferase* luminescent) by RNA silencing. Relative luciferase activity was increased in the IFN-treated cells compared to that in the untreated cells, meaning that IFN treatment decreased RNA silencing activity (Figure 8). However, RNA silencing activity in LGP2<sup>-/-</sup> HeLa cells treated with IFN was not decreased compared to that in WT HeLa cells, indicating that LGP2 functions to repress RNA silencing activity in normal condition.

The immunoprecipitation and luciferase assay revealed that LGP2 interacts with TRBP and represses RNA silencing activity, while other RLRs, RIG-I and MDA5, did not interact with TRBP. To investigate the contribution of the other RLRs on RNA silencing, RNA silencing activities were measured in WT HeLa cells



knocked down either of RIG-I or MDA5 using siRNAs against each gene (Figure 9, performed by Dr. Takahashi). Since AGO2 is an essential protein for RNA silencing, AGO2 was knocked down as a positive control. WT HeLa cells were treated with IFN and transfected with each siRNA (siAGO2, siRIG-I, siMDA5, and siLGP2). siRNA against GFP was used as a negative control, siCont. Plasmids encoding pre-miLuc, firefly *luciferase*, and *Renilla luciferase* were transfected into the cells and relative luciferase luminescent activity was measured. The protein level of each gene was sufficiently repressed by each specific siRNA (Figure 10). The knocking down of AGO2 increased relative luciferase activity, indicating that AGO2 functions to enhance RNA silencing activity. On the other hand, the knocking down of LGP2 or RIG-I decreased relative luciferase activity, indicating that not only LGP2 but also RIG-I function to repress RNA silencing activity (Figure 9). However, the knocking down of MDA5 did not decrease RNA silencing activity. Both RIG-I and LGP2 but not MDA5 can bind to short dsRNA, suggesting that RIG-I and LGP2 may sequester pre-miLuc and disturb RNA silencing by inhibition of miLuc maturation. Although LGP2 but not RIG-I interacted with TRBP (Figure 5), LGP2 can interact with RIG-I (Saito *et al.*, 2007), suggesting that RIG-I may affect TRBP-mediated RNA silencing activity through LGP2 indirectly.

To investigate whether RIG-I represses RNA silencing activity through LGP2 or not, RIG-I<sup>-/-</sup> HeLa cells were established using CRISPR/Cas9 system (Figure 11). sgRNA was designed against exon 1 of *rig-I* gene (Figure 11A). The mutation efficiency was 5.8 % in the *rig-I* region of the cells transfected with the sgRNA by T7EI assay (Figure 11B). The sgRNA-transfected cells were isolated by two rounds of limiting dilution and two patterns of mutation were detected in *rig-I* region by sequencing (Figure 11C). Signal of RIG-I protein was not observed in the cloned cell lysate by western blotting (Figure 11D). IFN-treated RIG-I<sup>-/-</sup> HeLa cells were transfected with each siRNA (siAGO2, siMDA5, and siLGP2) and RNA

silencing activity was measured (Figure 12). The protein level of each gene was sufficiently repressed by each specific siRNA (Figure 13). The knocking down of AGO2 increased relative luciferase activity. On the other hand, the knocking down of LGP2 significantly decreased relative luciferase activity, indicating that RIG-I is not necessary for the repression of RNA silencing activity by LGP2. Next, I measured RNA silencing activities in IFN-treated LGP2<sup>-/-</sup> HeLa cells with transfected with siRNA against each gene (Figure 14). The protein level of each gene was sufficiently repressed by each specific siRNA (Figure 15). The knocking down of AGO2 increased relative luciferase activity also in LGP2<sup>-/-</sup> HeLa cells. The knocking down of RIG-I little affected relative luciferase activity, suggesting that LGP2 may be necessary for the repression of RNA silencing by RIG-I.

The repression of RNA silencing activity by LGP2 and RIG-I is the result of RNA sequestration by them or TRBP interaction, RNA silencing activities were measured using IFN-treated TRBP<sup>-/-</sup> HeLa cells in which each gene was knocked down (Figure 16). The protein level of each gene was sufficiently repressed by each specific siRNA (Figure 17). The knocking down of AGO2 increased relative luciferase activity. On the other hand, knocking down of RIG-I and LGP2 were not changed in TRBP<sup>-/-</sup> HeLa cells, suggesting that RNA sequestration by LGP2 and RIG-I may have a little effect if any on RNA silencing activity, whereas LGP2 and RIG-I repressed RNA silencing activity through the interaction with TRBP. LGP2 but not RIG-I interacted with TRBP (Figure 5), whereas LGP2 can interact with RIG-I (Saito *et al.*, 2007). Thus, it was suggested that RIG-I regulates the function of TRBP indirectly through LGP2 and repressed RNA silencing activity. To investigate whether RIG-I can interact with TRBP indirectly through LGP2, TRBP was immunoprecipitated in WT HeLa cells transfected with different concentrations of a plasmid encoding RIG-I (performed by Dr. Takahashi). The result revealed that RIG-I can indirectly interact with TRBP through LGP2. Accordingly, it was considered

that RIG-I repressed RNA silencing activity by inhibiting the function of TRBP through LGP2.

It was revealed that LGP2 and RIG-I repress RNA silencing activity in human HeLa cells, which is derived from cervical cancer. To examine whether LGP2 and RIG-I repress RNA silencing activity in other human cells, I measured the effects of LGP2 and RIG-I on RNA silencing activity in human embryonic kidney-derived cell line, HEK293, with or without IFN treatment (Figure 18). In HEK 293 cells, IFN treatment increased relative luciferase activity, meaning that RNA silencing activity decreased. This result is the same as that in HeLa cells (Figure 9). Furthermore, the transfection of siLGP2 and siRIG-I decreased relative luciferase activity, indicating that LGP2 and RIG-I repressed RNA silencing activity also in HEK 293 cells (Figure 18). Thus, the repression of RNA silencing by LGP2 and RIG-I was conserved in different human cells.

### **2.3.3. Identification of TRBP-bound pre-miRNAs by RIP-sequencing analysis**

Given that knockdown of LGP2 in TRBP<sup>-/-</sup> HeLa cells did not affect RNA silencing activity, it was suggested that LGP2 represses RNA silencing activity through the interaction with TRBP. TRBP promotes RNA silencing by binding to pre-miRNAs and recruiting Dicer. The immunoprecipitation analysis showed that RNase treatment enhances LGP2-TRBP interaction and the dsRNA-binding sites in TRBP are efficient for interacting with LGP2 (performed by Dr. Takahashi). Therefore, it was considered that the interaction of LGP2 with TRBP releases pre-miRNAs bound to TRBP via the same sites of LGP2 binding, resulting in the repression of RNA silencing. However, it was unclear if TRBP regulates all types of pre-miRNAs or a particular type of miRNAs. To investigate whether TRBP has a specificity for pre-miRNA binding, I analyzed RIP-sequencing data whose library was prepared with Flp-In HEK293 cell line expressing N-terminal FLAG-tagged TRBP (established by

Dr. Takahashi and Mr. Murakami) by the steps shown in Figure 19, and normalized by reads per million mapped reads (RPM). The 562 pre-miRNAs were immunoprecipitated with TRBP. The enrichment rate by immunoprecipitation of each pre-miRNAs was calculated comparing with input RNAs, which are detected in the cell lysate not subjected to immunoprecipitation as follows: RPM of pre-miRNA in immunoprecipitates / RPM of pre-miRNA in input (Figure 20). The result showed that TRBP has a preference for binding to specific pre-miRNAs.

#### **2.3.4. Secondary structural features of TRBP-bound pre-miRNAs**

Generally, it is considered that dsRBDs do not display sequence-dependent RNA-binding (Vuković *et al.*, 2014). TRBP is known to be a dsRNA-binding protein which shows no sequence preference for small RNA-binding (Takahashi *et al.*, 2013). However, TRBP binds to dsRNA with perfect complementarity but not ssRNA, dsDNA, or DNA:RNA heteroduplex by the distinction of grooves width of duplex (Koh *et al.*, 2013, Vuković *et al.*, 2014). In addition, in vitro electrophoretic mobility shift assay (EMSA) demonstrated that TRBP's dsRNA binding affinity between miR-16-1 duplex mutants containing 1-nt mismatch and 1-nt bulge are different (Acevedo *et al.*, 2015). Therefore, I considered that TRBP's preference is caused by the difference in secondary structures of pre-miRNAs. Then, Top 40 pre-miRNAs (enrichment rate > 5) and Bottom 10 pre-miRNAs (enrichment rate < 1/3) were defined as TRBP-bound and TRBP-non-bound pre-miRNAs, respectively (Figure 20, Tables 5 and 6). To predict their secondary structures, pre-miRNA sequences were predicted using the data of miRNA database miRBase (Kozomara *et al.*, 2014). The secondary structures of each pre-miRNAs were predicted by CentroidFold, which is one of the most accurate tools for predicting secondary structure of RNA (Sato *et al.*, 2009). The CentroidFold predicts secondary structure by calculating base-pairing probability (bpp) which is a probability of each base

pairing with every base in RNA sequence. The mean value of the max bpp of each nucleotide in the pre-miRNA stem region calculated by CentroidFold was compared (Figure 21). All of 1761 human pre-miRNAs registered in miRBase were used as a control. The result showed that the bpp values of the TRBP-bound pre-miRNAs was significantly higher than control and that of TRBP-non-bound pre-miRNAs was tendency lower than control. On the other hand, the bpp values of the center in the stem region of both TRBP-bound and TRBP-non-bound pre-miRNAs were lower than control. The analysis revealed that the stem region of TRBP-bound pre-miRNAs contain tight base-pairing.

#### **2.3.5. The effect of LGP2 on maturation of TRBP-bound pre-miRNAs**

To examine the inhibitory effect of LGP2 on the maturation of TRBP-bound pre-miRNAs, the mature miRNA levels of a TRBP-bound pre-miR-106b and a TRBP-non-bound pre-miR-19b were measured in WT or LGP2<sup>-/-</sup> HeLa cells by RT-PCR. The amounts of mature miR-106b in LGP2<sup>-/-</sup> HeLa cells was higher than that in WT HeLa cells (Figure 22A). On the other hand, the amount of mature miR-19b was not changed (Figure 22B). In addition, mature miRNA level of miR-106b were detected in WT or LGP2<sup>-/-</sup> HeLa cells transfected with a plasmid encoding LGP2 at different concentrations by RT-PCR. First, I confirmed that mRNA level of LGP2 was increase according to the concentrations of LGP2 transfection (Figure 23A). The overexpression of LGP2 at different concentrations in LGP2<sup>-/-</sup> HeLa cells decreased the mature miRNA level of miR-106b in a concentration-dependent manner of LGP2 (Figure 23B). These results showed that LGP2 may inhibit maturation of TRBP-bound pre-miRNAs. Further immunoprecipitation assay represented that LGP2 interacts with TRBP via its ATPase/Helicase domain (performed by Dr. Takahashi). ATPase/Helicase domain ( $\Delta$ CTD) or CTD of LGP2 was expressed in LGP2<sup>-/-</sup> HeLa cells and mature miRNA level of miR-106b was measured by RT-PCR (Figure 22A).

The expression of CTD lacking the TRBP-interacting region increased the mature miRNA level of miR-106b compared to that of ATPase/Helicase domain, indicating that ATPase/Helicase domain is sufficient to repress the maturation of miR-106b.

#### **2.3.6. The effect of LGP2 on target mRNA levels of mature miRNA biosynthesized from TRBP-bound pre-miRNAs**

LGP2 repressed the maturation of miR-106b, one of the TRBP-bound pre-miRNAs, by the interaction with TRBP, suggesting that the expression of genes targeted by miR-106b is upregulated. Thereby, the genes targeted by miR-106b and miR-19b were predicted by TargetScan (Agarwal *et al.*, 2015), respectively. The expression of the predicted target genes was measured in WT or LGP2<sup>-/-</sup> HeLa cells by qRT-PCR. In LGP2<sup>-/-</sup> HeLa cells, the predicted target genes of miR-106b, DERL2 and ZNFX1, were significantly decreased (Figure 24). On the other hand, the predicted target genes of miR-19b, QKI and RAB18, were not changed or slightly increased (Figure 25). Furthermore, when a plasmid encoding miR-106b inhibitor (TuD-miR-106b) was transfected into LGP2<sup>-/-</sup> HeLa cells, the expression of ZNFX1 was recovered, suggesting that LGP2 inhibits RNA silencing by repressing the maturation of miR-106b and upregulates its target genes, as a result of its TRBP interaction (Figure 24).

#### **2.4. Discussion**

Although LGP2 is a member of virus sensor RLRs family proteins, the function of LGP2 in RLR signaling was unclear due to a lack of CARD which is essential for downstream signaling. However, the result of immunoprecipitation suggested that LGP2 regulates RNA silencing by interacting with TRBP. To examine the effect of LGP2 on RNA silencing, dual-luciferase assay was performed in different cell lines with IFN treatment. The result represented that LGP2 represses RNA silencing via TRBP (Figures 8 and 16). In RNA silencing pathway, TRBP enhances RNA silencing by binding to pre-miRNAs, recruiting

Dicer to them, and promoting the processing by Dicer. Therefore, LGP2 was considered to disturb TRBP's binding to pre-miRNAs by interacting with TRBP. According to this hypothesis, it was suggested that LGP2 downregulates miRNAs regulated by TRBP and upregulates their target genes. The result of RIP-sequencing indicated that TRBP binds to specific pre-miRNAs (Figure 20). By predicting secondary structures of TRBP-bound and TRBP-non-bound pre-miRNAs using CentroidFold, I found that TRBP-bound pre-miRNAs include the stem region with tight base pairing (Figure 21). Moreover, RT-PCR showed that LGP2 decreased mature miRNA level of a TRBP-bound miRNA, miR-106b, and increased mRNA level of its targets, DERL2 and ZNFX1 (Figures 22-24). On the other hand, LGP2 hardly affected mature miRNA level of a TRBP-non-bound miRNA, miR-19b, and mRNA level of its targets, QKI and RAB18 (Figures 22 and 25). Therefore, LGP2 may regulate the expression of genes targeted by specific miRNAs mediated by TRBP.

In RNA silencing, miRNAs downregulate specific genes by destabilization or translational repression of their mRNAs. The only 7-nt of “seed” sequence at positions 2-8 nt from 5' end of miRNA acts as a target recognition site. Therefore, a miRNA regulates a large number of genes containing seed complementary sequences coincidentally. In this study, LGP2 was considered to downregulate a group of miRNAs mediated by TRBP. LGP2 repressed the maturation of TRBP-bound miR-106b (Figure 22 and 23), which promotes cell proliferation and inhibits apoptosis by the negative regulation of a tumor suppressor B-cell translocation gene anti-proliferation factor 3 (BTG3) (Wei *et al.*, 2017). Furthermore, TRBP-bound miRNAs contain many miRNAs relating to cell proliferation or cell death (e.g., miR-31, miR-25, miR-140, miR-582, miR-340, miR-16-1, and miR-10b). Thus, LGP2 may regulate cell proliferation or cell death by interacting with TRBP.

第3章については、5年以内に雑誌などで刊行予定のため、非公開。



## 4. Conclusion

Mammalian cells have two different mechanisms induced by dsRNA in the cytoplasm. One is antiviral response induced through RLRs which detect exogenous dsRNAs such as viral RNAs. The other is RNA silencing triggered by endogenous small non-coding RNAs, miRNAs. Although both pathways are triggered by dsRNAs in the cytoplasm, the crosstalk mechanism between them remained unidentified.

In Chapter 2, I found that one of RLRs, LGP2 interacts with an RNA silencing enhancer TRBP. Although LGP2 is a member of RLRs, virus sensors, its function in RLR signaling remains unclear because of lacking CARD which can transduce the downstream signaling for IFN induction. The function of TRBP in RNA silencing also remains unclear, since TRBP was considered to enhance RNA silencing mediated by any miRNAs, but RNA silencing occurs without TRBP. However, I discovered that TRBP has a structural preference on miRNA-binding, and LGP2 regulates expression of particular genes by interaction with TRBP. Since TRBP binds to LGP2 via its dsRNA-binding sites, TRBP cannot bind to pre-miRNA upon LGP2 interaction, and RNA silencing mediated by TRBP-bound miRNAs is repressed. Accordingly, the findings indicate that LGP2 and TRBP play an important role in gene network regulation by interacting each other.

5年以内に雑誌などで刊行予定のため、非公開。

## **Acknowledgement**

I would like to express my appreciation for my supervisor Professor Dr. Kumiko Ui-Tei. I would like to thank you for your excellent detailed guidance. Without the guidance and help, this dissertation would not have been possible. I would also like to thank assistant professor Tomoko Takahashi for giving me useful suggestion and knowledge.

I also thank Dr. M. Yoneyama and Dr. K. Onomoto for providing helpful comments and poly(I:C), Dr. H. Iba and Dr. T. Hamaguchi for providing miRNA inhibitor (TuD-decoy), and Dr. Y. Suzuki for performing RNA sequencing.

## References

- Acevedo R., Orench-RiVera N., Quarles KA., and Showalter SA. (2015) Helical defects in microRNA influence protein binding by TAR RNA binding protein. *PLoS One.*, **10**, e0116749.
- Agarwal V., Bell GW., Nam JW., and Bartel DP. (2015) Predicting effective microRNA target sites in mammalian mRNAs. *Elife.*, **4**, e05005.
- Alenzi FQ. (2004) Links between apoptosis, proliferation, and the cell cycle. *Br J Biomed Sci.*, **61**, 99-102.
- Anders S., Pyl P.T. and Huber W. (2015) HTSeq-a Python framework to work with high-throughput sequencing data. *Bioinformatics*, **31**, 166-169.
- Andrews S. (2010) FastQC: a quality control tool for high throughput sequence data. Available online at: <http://www.bioinformatics.babraham.ac.uk/projects/fastqc>
- Bannwarth S., Talakoub L., Letourneur F., Duarte M., Purcell DF., Hiscott J. and Gatignol A. (2001) Organization of the human *tarbp2* gene reveals two promoters that are repressed in an astrocytic cell line. *J Biol Chem.*, **276**, 48803-48813.
- Bartel DP. (2004) MicroRNAs: genomics, biogenesis, mechanism, and function. *Cell.*, **116**, 281-297.
- Beckham SA., Brouwer J., Roth A., Wang D., Sadler AJ., John M., Jahn-Hofmann K., Williams BR., Wilce JA., and Wilce MC. (2013) Conformational rearrangement of RIG-I receptor on formation of a multiprotein:dsRNA assembly. *Nucleic Acids Res.*, **41**, 3436-3445.

Bohnsack MT., Czaplinski K. and Gorlich D. (2004) Exportin 5 is a RanGTP-dependent dsRNA-binding protein that mediates nuclear export of pre-miRNAs. *RNA.*, **10**, 185-181.

Brady HJ., Gil-Gómez G., Kirberg J., and Berns AJ. (1996) Bax alpha perturbs T cell development and affects cell cycle entry of T cells. *EMBO J.*, **15**, 6991-7001.

Cassimere EK., Mauvais C., and Denicourt C. (2016) p27Kip1 Is Required to Mediate a G1 Cell Cycle Arrest Downstream of ATM following Genotoxic Stress. *PLoS One.*, **11**, e0162806.

Chakravarthy S., Stemberg SH., Kellenberger CA., and Doudna JA. (2010) Substrate-specific kinetics of Dicer-catalyzed RNA processing. *J Mol Biol.*, **404**, 392-402.

Chen H., Wang DL., and Liu YL. (2016) Poly (I:C) transfection induces mitochondrial-mediated apoptosis in cervical cancer. *Mol Med Rep.*, **13**, 2689-2695.

Chendrimada TP., Gregory RI., Kumaraswamy E., Norman J., Cooch N., Nishikura K. and Shiekhattar R. (2005) TRBP recruits the Dicer complex to Ago2 for microRNA processing and gene silencing. *Nature.*, **436**, 740-744.

Croce CM. (2009) Causes and consequences of microRNA dysregulation in cancer. *Not Rev Genet.*, **10**, 704-714.

Cuadrado M., Gutierrez-Martinez P., Swat A., Nebreda AR., and Fernandez-Capetillo O. (2009) p27Kip1 stabilization is essential for the maintenance of cell cycle arrest in response to DNA damage. *Cancer Res.*, **69**, 8726-8732.

Cui S., Eisenächer K., Kirchhofer A, Brzózka K, Lammens A, Lammens K, Fujita T, Conzelmann KK, Krug A, and Hopfner KP. (2008) The C-terminal regulatory domain is the RNA 5'-triphosphate sensor of RIG-I. *Mol Cell.*, **29**, 169-179.

Daniels SM., Melendez-Peña CE., Scarborough RJ., Daher A., Christensen HS., El Far M., Purcell DF., Lainé S. and Gatignol A. (2009) Characterization of the TRBP domain required for dicer interaction and function in RNA interference. *BMC Mol Biol.*, **10**.

Doi N., Zenno S., Ueda R., Ohki-Hamazaki H., Ui-Tei K., and Saigo K. (2003) Short-interfering-RNA-mediated gene silencing in mammalian cells requires Dicer and eIF2C translation initiation factors. *Curr Biol.*, **13**, 41-46.

Doyle S., Vaidya S., O'Connell R., Dadgostar H., Dempsey P., Wu T., Rao G., Sun R., Haberland M., Modlin R., and Cheng G. (2002) IRF3 mediates a TLR3/TLR4-specific antiviral gene program. *Immunity.*, **17**, 251-263.

Duarte M., Graham K., Daher A., Battisti PL., Bannwarth S., Segeral E., Jeang KT. and Gatignol A. (2000) Characterization of TRBP1 and TRBP2. Stable stem-loop structure at the 5' end of TRBP2 mRNA resembles HIV-1 TAR and is not found in its processed pseudogene. *J Biomed Sci.*, **7**, 494-506.

Fang R., Jiang Q., Zhou X., Wang C., Guan Y., Tao J., Xi J., Feng JM., Jiang Z. (2017) MAVS activates TBK1 and IKKε through TRAFs in NEMO dependent and independent manner. *PLoS Pathog.*, **13**, e1006720.

Fareh M., Yeom KH., Haagsma AC., Chauhan S., Heo I., and Joo C. (2016) TRBP ensures efficient Dicer processing of precursor microRNA in RNA-crowded environments. *Nat Commun.*, **7**, 13694.

Gatignol A., Buckler-White A., Berkhout B. and Jeang KT. (1991) Characterization of a human TAR RNA-binding protein that activates the HIV-1 LTR. *Science*, **251**, 1597-1600.

Gil-Gómez G., Berns A., and Brady HJ. (1998) A link between cell cycle and cell death: Bax and Bcl-2 modulate Cdk2 activation during thymocyte apoptosis. *EMBO J.*, **17**, 7209-7218.

Gleghorn ML. and Maquat LE. (2014) ‘Black sheep’ that don’t leave the double-stranded RNA-binding domain fold. *Trends Biochem Sci.*, **37**, 328-340.

Goubau D., Schlee M., Deddouche S., Pruijsers AJ., Zillinger T., Goldeck M., Schuberth C., Van der Veen AG., Fujimura T., Rehwinkel J., Iskarpatyoti JA., Barchet W., Ludwig J., Dermody TS., Hartmann G., and Reis e Sousa C. (2014) Antiviral immunity via RIG-I-mediated recognition of RNA bearing 5'-diphosphates. *Nature.*, **514**, 372-375.

Griggiths-Jones S., Grocock RJ., Van Dongen S., Bateman A. and Enright AJ. (2006) miRBase: microRNA sequences, targets and gene nomenclature. *Nucleic Acids Res.*, **34**, D140-144.

Grimson A., Farth KK., Johnston WK., Garrett-Engle P., Lim LP., and Bartel DP. (2007) MicroRNA targeting specificity in mammals: determinants beyond seed pairing. *Mol Cell.*, **27**, 91-105.

Haase AD., Jaskiewicz L., Zhang H., Laine S., Sack R., Gatignol A. and Filipowicz W. (2005) TRBP, a regulator of cellular PKR and HIV-1 virus expression, interacts with Dicer and functions in RNA silencing. *EMBO Rep.*, **6**, 961-967.

Han H., Shim H., Shin D., Shim JE., Ko Y., Shin J., Kim H., Cho A., Kim E., Lee T., Kim H., Kim K., Yang S., Bae D., Yun A., Kim S., Kim CY., Cho HJ., Kang B., Shin S., and Lee I. (2015) TRRUST: a reference database of human transcriptional regulatory interactions. *Sci Rep.*, **5**, 11432.

- Han J., Lee Y., Yeom KH., Nam JW., Heo I., Rhee JK., Sohn SY., Cho Y., Zhang BT., and Kim VN. (2006) Molecular Basis for the Recognition of Primary microRNAs by the Drosha-DGCR8 Complex. *Cell*. **125**, 887-901.
- Haraguchi T., Ozaki Y., and Iba H. (2009) Vectors expressing efficient RNA decoys achieve the long-term suppression of specific microRNA activity in mammalian cells. *Nucleic Acids Res.*, **37**, e43.
- Hauber J. and Cullen BR. (1988) Mutational analysis of the trans-activation-responsive region of the human immunodeficiency virus type I long terminal repeat. *J Virol.*, **62**, 673-679.
- Huang DW., Sherman BT., and Lempicki RA. (2009) Systematic and integrative analysis of large gene lists using DAVID Bioinformatics Resources. *Nature Protoc.*, **4**, 44-57.
- Huang DW., Sherman BT., Lempicki RA. (2009) Bioinformatics enrichment tools: paths toward the comprehensive functional analysis of large gene lists. *Nucleic Acids Res.*, **37**, 1-13.
- Hornung V., Ellegast J., Kim S., Brzózka K., Jung A., Kato H., Poeck H., Akira S., Conzeimann KK., Schlee M., Endres S., and Hartmann G. (2006) 5'-Triphosphate RNA is the ligand for RIG-I. *Science*., **314**, 994-997.
- Kato H., Takeuchi O., Mikamo-Satoh E., Hirai R., Kawai T., Matsushita K., Hiiragi A., Dermody TS., Fujita T., and Akira S. (2008) Length-dependent recognition of double-stranded ribonucleic acids by retinoic acid-inducible gene-I and melanoma differentiation-associated gene 5. *J Exp Med.*, **205**, 1601-1610.
- Kim Y., Yeo J., Lee JH., Cho J., Seo D., Kim JS., and Kim VN. (2014) Deletion of human tarbp2 reveals cellular microRNA targets and cell-cycle function of TRBP. *Cell Rep.*, **9**, 1061-1074.

Koh HR., Kidwell MA., Ragunathan K., Doudna JA., and Myong S. (2013) ATP-independent diffusion of double-stranded RNA binding proteins. *Proc Natl Acad Sci U S A.*, **110**, 151-156.

Kowalinski E., Lunardi T., McCarthy AA., Louber J., Brunel J., Grigorov B., Gerlier D., and Cusack S. (2011) Structural basis for the activation of innate immune pattern-recognition receptor RIG-I by viral RNA. *Cell.*, **147**, 423-435.

Kozomara A. and Griffiths-Jones S. (2014) miRBase: annotating high confidence microRNAs using deep sequencing data. *Nucleic Acids Res.*, **42**, D68-73.

Kwon SC., Nguyen TA., Choi YG., Jo MH., Hohng S., Kim VN., and Woo J.S. (2016) Structure of human Drosha. *Cell.*, **164**, 81-90.

Lee Y., Kim M., Han J., Yeom KH., Lee S., Baek SH., and Kim VN. (2004) MicroRNA genes are transcribed by RNA polymerase II. *EMBO J.*, **13**, 4051-4060.

Lee Y., Ahn C., Han J., Choi H., Kim J., Lee J., Provost P., Rådmark O., Kim S. and Kim VN. (2003) The nuclear RNase III Drosha initiates microRNA processing. *Nature*, **425**, 415-419.

Lim LP., Lau NC., Garrett-Engle P., Grimson A., Schelter JM., Castle J., Bartel DP., Linsley PS., and Johnson JM. (2005) Microarray analysis shows that some microRNAs downregulate large numbers target mRNAs. *Nature.*, **433**, 769-773.

Liu J., Carmell MA., Rivas FV., Marsden CG., Thomson JM., Song JJ., Hammond SM., Joshua-Tor L., and Hannon GJ. (2004) Argonaute2 is the catalytic engine of mammalian RNAi. *Science.*, **305**, 1437-1441.



- Liu L., Botos I., Wang Y., Leonard JN., Shiloach J., Segal DM., and Davies DR. (2008) Structural basis of toll-like receptor 3 signaling with double-stranded RNA. *Science.*, **320**, 379-381.
- MacRae IJ., Ma E., Zhou M., Robinson CV., and Doudna JA. (2008) In vitro reconstitution of the human RISC-loading complex. *Proc Natl Acad Sci U S A.*, **105**, 512-517.
- Malathi K., Dong B., Gale M Jr., and Silverman RH. (2007) Small self-RNA generated by RNase L amplifies antiviral innate immunity. *Nature.*, **448**, 816-819.
- Maniatakis E., and Mourelatos Z. (2005) A human, ATP-independent, RISC assembly machine fueled by pre-miRNA. *Genes Dev.*, **19**, 2979-2990.
- Nishiya T., and DeFranco AL. (2004) Ligand-regulated chimeric receptor approach reveals distinctive subcellular localization and signaling properties of the Toll-like receptors. *J Biol Chem.*, **279**, 19008-19017.
- Marcel M. (2012) Cutadapt removes adapter sequences from high-throughput sequencing reads. *Bioinformatics in Action.*, **17**, 10-12.
- Marq JB., Hausmann S., Veillard N., Kolakofsky D., Garcin D. (2011) Short double-stranded RNAs with an overhang 5' ppp-nucleotide, as found in arenavirus genomes, act as RIG-I decoys. *J. Biol. Chem.*, **286**, 6108-6116.
- Naito Y., Hino K., Bono H., and Ui-Tei K. (2015) CRISPRdirect: software for designing CRISPR/Cas guide RNA with reduced off-target sites. *Bioinformatics.*, **31**, 1120-1123.
- Narita R., Takahashi K., Murakami E., Hirano E., Yamamoto SP., Yoneyama M., Kato H. and Fujita T. (2014) A novel function of human Puvilio proteins in cytoplasmic sensing of viral infection. *PLoS Pathog.*, **10**, e1004417.

Nguyen TA., Jo MH., Choi YG., Park J., Kwon SC., Hohng S., Kim VN., and Woo JS. (2015) Functional anatomy of the human Microprocessor. *Cell.*, **161**, 1374-1387.

Okada-Katsuhata Y., Yamashita A., Kutsuzawa K., Izumi N., Hirahara F., and Ohno S. (2012) N- and C-terminal Upf1 phosphorylation create binding platforms for SMG-6 and SMG-5:SMG-7 during NMD. *Nucleic Acids Res.*, **40**, 1251-1266.

Pathak HB., Ghosh SK., Roberts AW., Sharma SD., Yoder JD., Arnold JJ., Gohara DW., Barton DJ., Paul AV., and Cameron CE. (2002) Structure-function relationships of the RNA-dependent RNA polymerase from poliovirus (3Dpol). A surface of the primary oligomerization domain functions in capsid precursor processing and VPg uridylylation. *J Biol Chem.*, **277**, 31551-31562.

Peng S., Geng J., Sun R., Tian Z., and Wei H. (2009) Polyinosinic-polycytidylic acid liposome induces human hepatoma cells apoptosis which correlates to the up-regulation of RIG-I like receptors. *Cancer Sci.*, **100**, 529-536.

Provost P., Dishart D., Doucet J., Frendewey D., Samuelsson B., and Rådmark O. (2002) Ribonuclease activity and RNA binding of recombinant human Dicer. *EMBO J.*, **21**, 5864-5874.

Rehwinkel J., Tan CP., Goubau D., Schulz O., Pichlmair A., Bier K., Robb N., Vreede F., Barclay W., Fodor E., and Reis e Sousa C. (2010) RIG-I detects viral genomic RNA during negative-strand RNA virus infection. *Cell.*, **140**, 397-408.

Rothenfusser S., Goutagny N., DiPerna G., Gong M., Monks BG., Schoenemeyer A., Yamamoto M., Akira S., and Fitzgerald KA. (2005) The RNA helicase Lgp2 inhibits TLR-independent sensing of viral replication by retinoic acid-inducible gene-I. *J Immunol.*, **175**, 5260-5268.

Sadler AJ., and Williams BR. (2008) Interferon-inducible antiviral effectors. *Nat Rev Immunol.*, **8**, 559-568.

Saha SK., Pietras EM., He JQ., Kang JR., Liu SY., Oganessian G., Shahangian A., Zarnegar B., Shiba TL., Wang Y., Cheng G. (2006) Regulation of antiviral responses by a direct and specific interaction between TRAF3 and Cardif. *EMBO J.*, **25**, 3257-3263.

Saito T., Hirai R., Loo YM., Owen D., Johnson CL., Sinha SC., Akira S., Fujita T., and Gale M Jr. (2007) Regulation of innate antiviral defenses through a shared repressor domain in RIG-I and LGP2. *Proc Natl Acad Sci U S A.*, **104**, 582-587.

Sato K., Hamada M., Asai K. and Mituyama T. (2009) CENTROIDFOLD: a web server for RNA secondary structure prediction. *Nucleic Acids Res.*, **37**, W277-W280.

Sato S., Sugiyama M., Yamamoto M., Watanabe Y., Kawai T., Takeda K., and Akira S. (2003) Toll/IL-1 receptor domain-containing adaptor inducing IFN-beta (TRIF) associates with TNF receptor-associated factor 6 and TANK-binding kinase 1, and activates two distinct transcription factors, NF-kappa B and IFN-regulatory factor-3, in the Toll-like receptor signaling. *J Immunol.*, **171**, 4304-4310.

Schlee M., Roth A., Hornung V., Hagmann CA., Wilmmenauer V., Barchet W., Coch C., Janke M., Mihailovic A., Wardle G., Juranek S., Kato H., Kawai T., Poeck H., Fitzgerald KA., Takeuchi O., Akira S., Tischi T., Latz E., Ludwig J., and Hartmann G. (2009) Recognition of 5' triphosphate by RIG-I helicase requires short blunt double-stranded RNA as contained in panhandle of negative-strand virus. *Immunity.*, **31**, 25-34.

St Johnston D., Brown NH., Gall JG. and jantsch M. (1992) A conserved double-stranded RNA-binding domain. *Proc Natl Acad Sci U S A.*, **89**, 10979-10983.

Su H., Trombly MI., Chen J., and Wang X. (2009) Essential and overlapping functions for mammalian Argonautes in microRNA silencing. *Genes Dev.*, **23**, 304-317.

Takahashi T., Miyakawa T., Zenno S., Nishi K., Tanokura M. and Ui-Tei K. (2013) Distinguishable in vitro binding mode of monomeric TRBP and dimeric PACT with siRNA. *PLoS One.*, **8**, e63434.

Takahashi T., Zenno S., Ishibashi O., Takizawa T., Saigo K., and Ui-Tei K. (2014) Interactions between the non-seed region of siRNA and RNA-binding RLC/RISC proteins, Ago and TRBP, in mammalian cells. *Nucleic Acids Res.*, **42**, 5256-5269.

Ui-Tei K., Naito Y., Takahashi F., Haraguchi T., Ohki-Hamazaki H., Juni A., Ueda R., and Saigo K. (2004) Guidelines for the selection of highly effective siRNA sequences for mammalian and chick RNA interference. *Nucleic Acids Res.*, **32**, 936–948.

Ui-Tei K., Maruyama S., and Nakano Y. (2017) Enhancement of single guide RNA transcription for efficient CRISPR/Cas-based genomic engineering. *Genome.*, **60**, 537-545.

Vuković L., Koh HR., Myong S., and Schulten K. (2014) Substrate recognition and specificity of double-stranded RNA binding proteins. *Biochemistry.*, **53**, 3457-3466.

Wang HW., Noland C., Siridechadilok B., Taylor DW., Ma E., Felderer K., Doudna JA., and Nogales E. (2009) Structural insights into RNA processing by the human RISC-loading complex. *Nat Struct Mol Biol.*, **16**, 1148-1153.

Wang X., Gorospe M., Huang Y., and Holbrook NJ. (1997) p27Kip1 overexpression causes apoptotic death of mammalian cells. *Oncogene.*, **15**, 2991-2997.

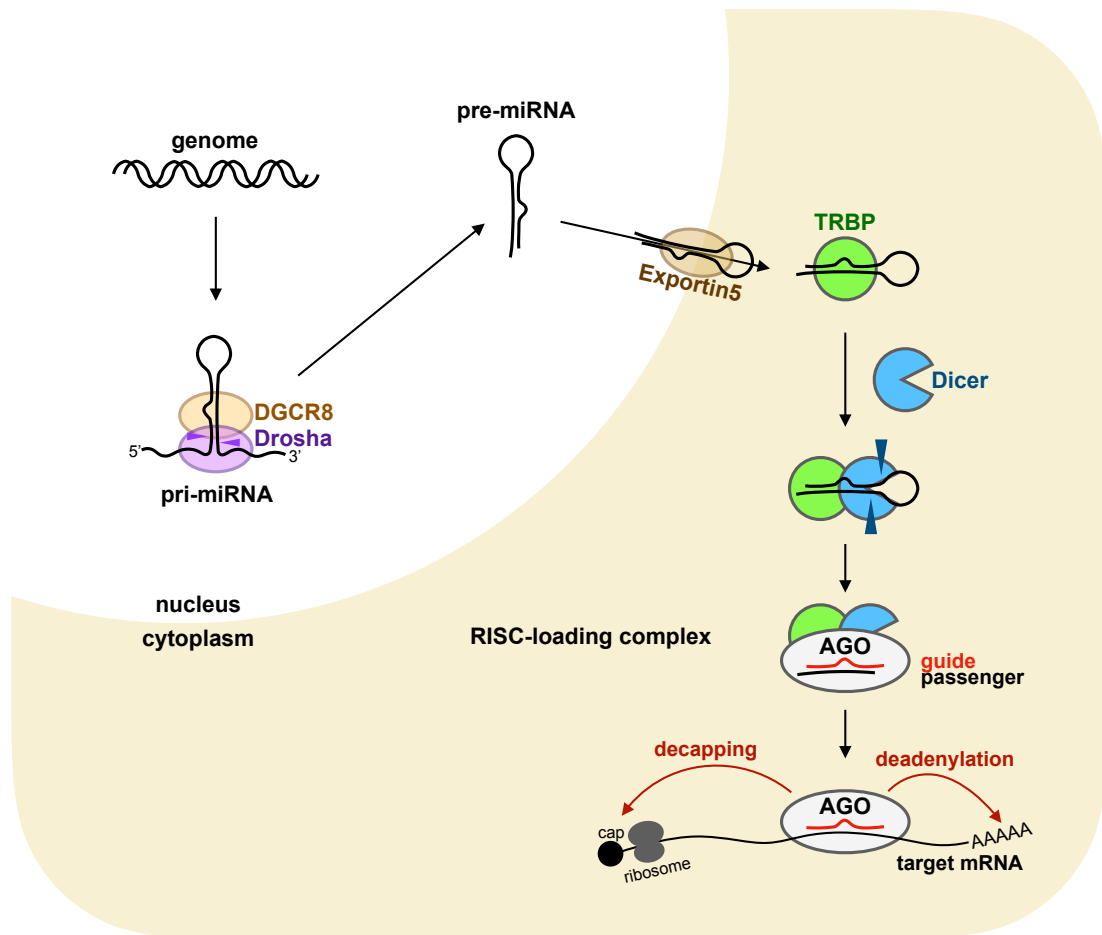
Wei K., Pan C., Yao G., Liu B., Ma T., Xia Y., Jiang W., Chen L., and Chen Y. (2017) MiR-106b-5p promotes proliferation and inhibits apoptosis by regulating BTG3 in non-small cell lung cancer. *Cell Physiol Biochem.*, **44**, 1545-1558.

Wilson RC., Tambe A., Kidwell MA., Noland CL., Schneider CP., and Doudna JA. (2015) Dicer-TRBP complex formation ensures accurate mammalian microRNA biogenesis. *Mol Cell.*, **57**, 397-407.

Yi R., Qin Y., Macara IG. and Cullen BR. (2003) Exportin-5 mediates the nuclear export of pre-microRNAs and short hairpin RNAs. *Genes Dev.*, **17**, 3011-3016.

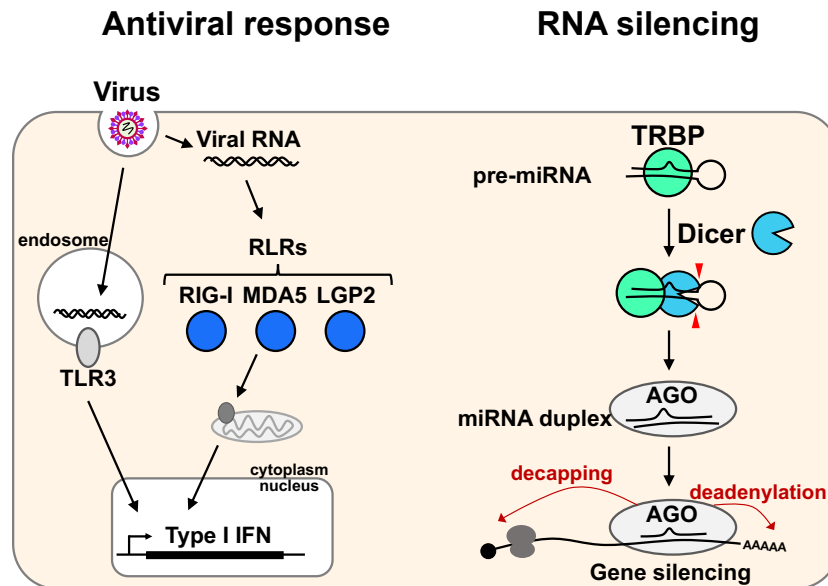
Yoneyama M., Kikuchi M., Natsukawa T., Shinobu N., Imaizumi T., Miyagishi M., Taira K., Akira S., and Fujita T. (2004) The RNA helicase RIG-I has an essential function in double-stranded RNA-induced innate antiviral responses. *Nat Immunol.*, **5**, 730-737.

Yoneyama M., Kikuchi M., Matsumoto K., Imaizumi T., Miyagishi M., Taira K., Foy E., Loo YM., Gale M Jr., Akira S., Yonehara S., Kato A., Fujita T. (2005) Shared and unique functions of the DExD/H-box helicases RIG-I, MDA5, and LGP2 in antiviral innate immunity. *J Immunol.*, **175**, 2851-2858.



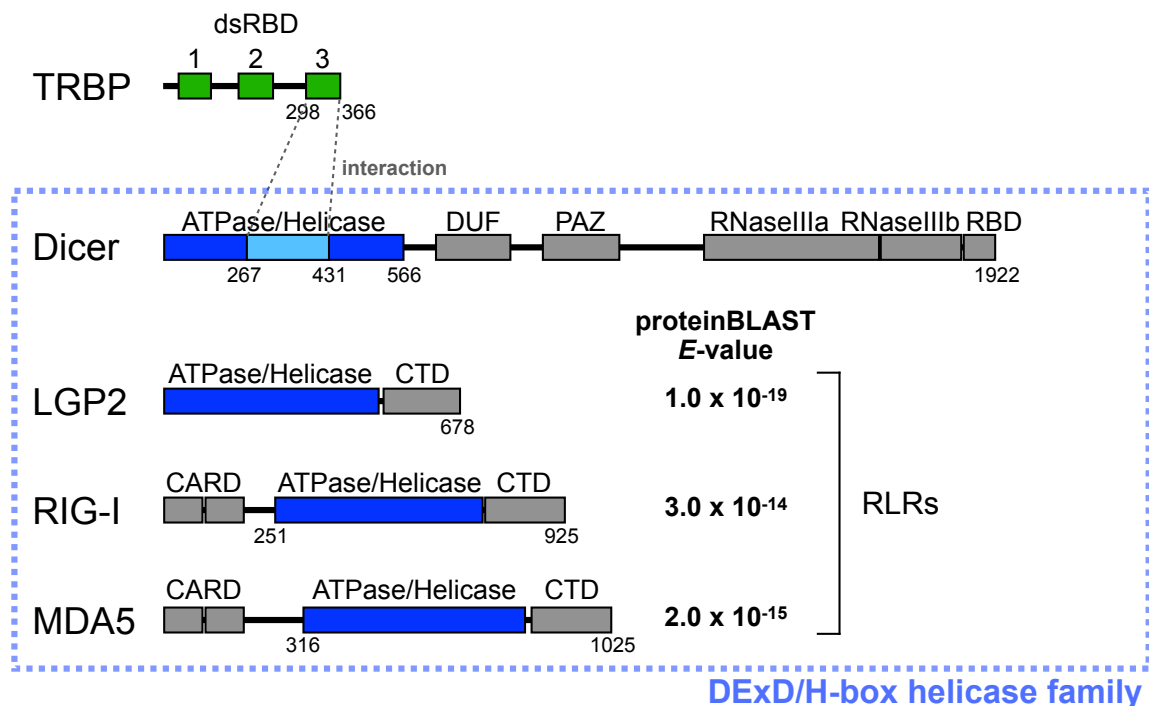
**Figure.1 RNA silencing pathway in human cells.**

miRNAs are transcribed from genome as pri-miRNAs and processed into pre-miRNAs by Drosha and DGCR8 complex in the nucleus. The pre-miRNAs are exported into the cytoplasm via Exportin5. TRBP binds to pre-miRNAs and recruits Dicer to promote the processing into miRNA duplexes. The miRNA duplex loads onto AGO contained in RLC. The miRNA duplex unwinds into single-stranded RNA within AGO. One strand of them (guide strand) binds to target mRNA with complementary sequence, resulting gene silencing by translational repression of target mRNAs through decapping and/or deadenylation.



## Figure.2 Antiviral response and RNA silencing

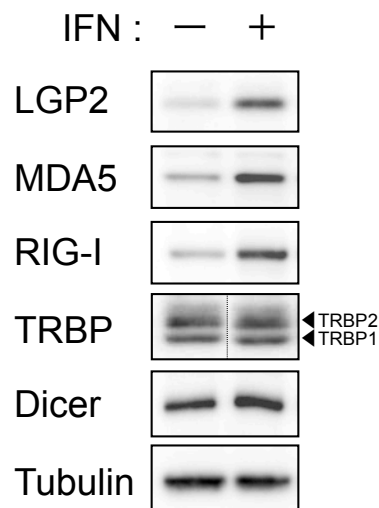
In mammalian cells, both antiviral response and RNA silencing are triggered by dsRNA in the cytoplasm. (Left) During virus infection, viral RNAs are detected by the host PRRs (RIG-I, MDA5, LGP2, TLR3), and type I interferon production is induced. RLRs and TLR3 function as intracellular PRRs in the cytoplasm and endosome, respectively. (Right) In RNA silencing, pre-miRNA binds to an RNA silencing enhancer, TRBP, which recruits Dicer to process pre-miRNA into miRNA duplex. The miRNA duplex loads onto AGO and unwind into single strands. One strand of them (guide strand) binds to target mRNA with complementary sequence to silence its expression.



**Figure.3 Domain structures of TRBP, Dicer, and RLRs (LGP2, RIG-I, and MDA5).**

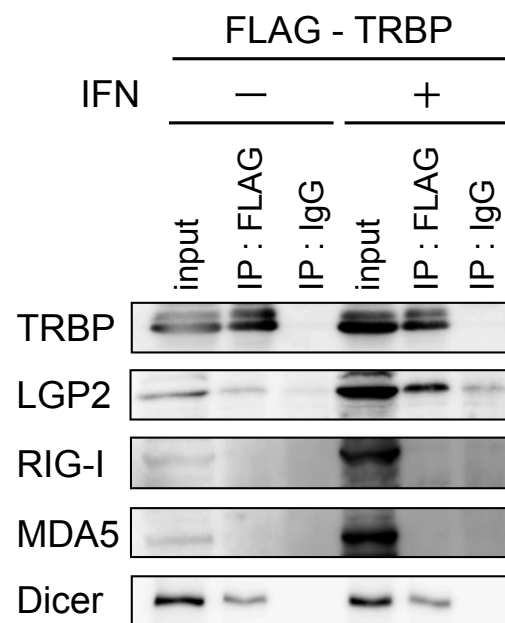
TRBP is a dsRNA binding protein which consists of three dsRBDs. N-terminal dsRBD1 and dsRBD2 are necessary for binding to dsRNAs and C-terminal dsRBD3 is involved in interacting with other proteins. Dicer is an endoribonuclease which consists of ATPase/Helicase, DUF, PAZ, two RNaseIII domains, and RBD. TRBP interacts with the amino acid region 267-431 in Dicer via its dsRBD3. RIG-I and MDA5 share similar domain structure, ATPase/Helicase domain, and CTD. However, LGP2 lacks the CARDs. All RLRs and Dicer are members of a DExD/H-box RNA helicase family protein.





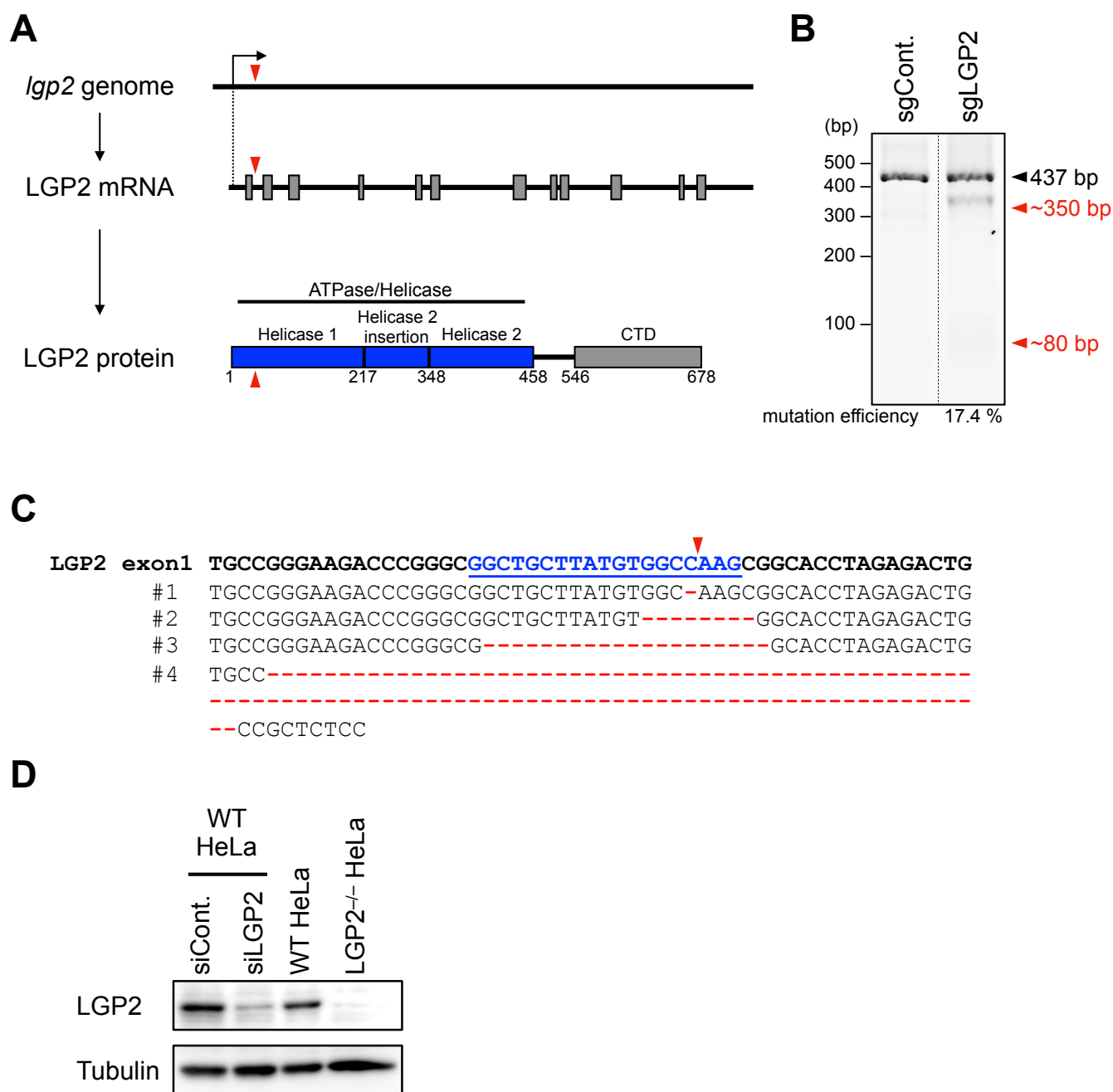
**Figure.4 Western blots of RLRs (LGP2, RIG-I, and MDA5) and RNA silencing factors (TRBP and Dicer) with or without IFN treatment.**

Western blots of RLRs (LGP2, RIG-I, and MDA5) and RNA silencing factors (TRBP and Dicer) in HeLa cells with or without IFN treatment. Each endogenous protein was detected with specific antibody. Tubulin was used as a control. IFN treatment induced the expression of all RLRs, but not that of TRBP and Dicer.



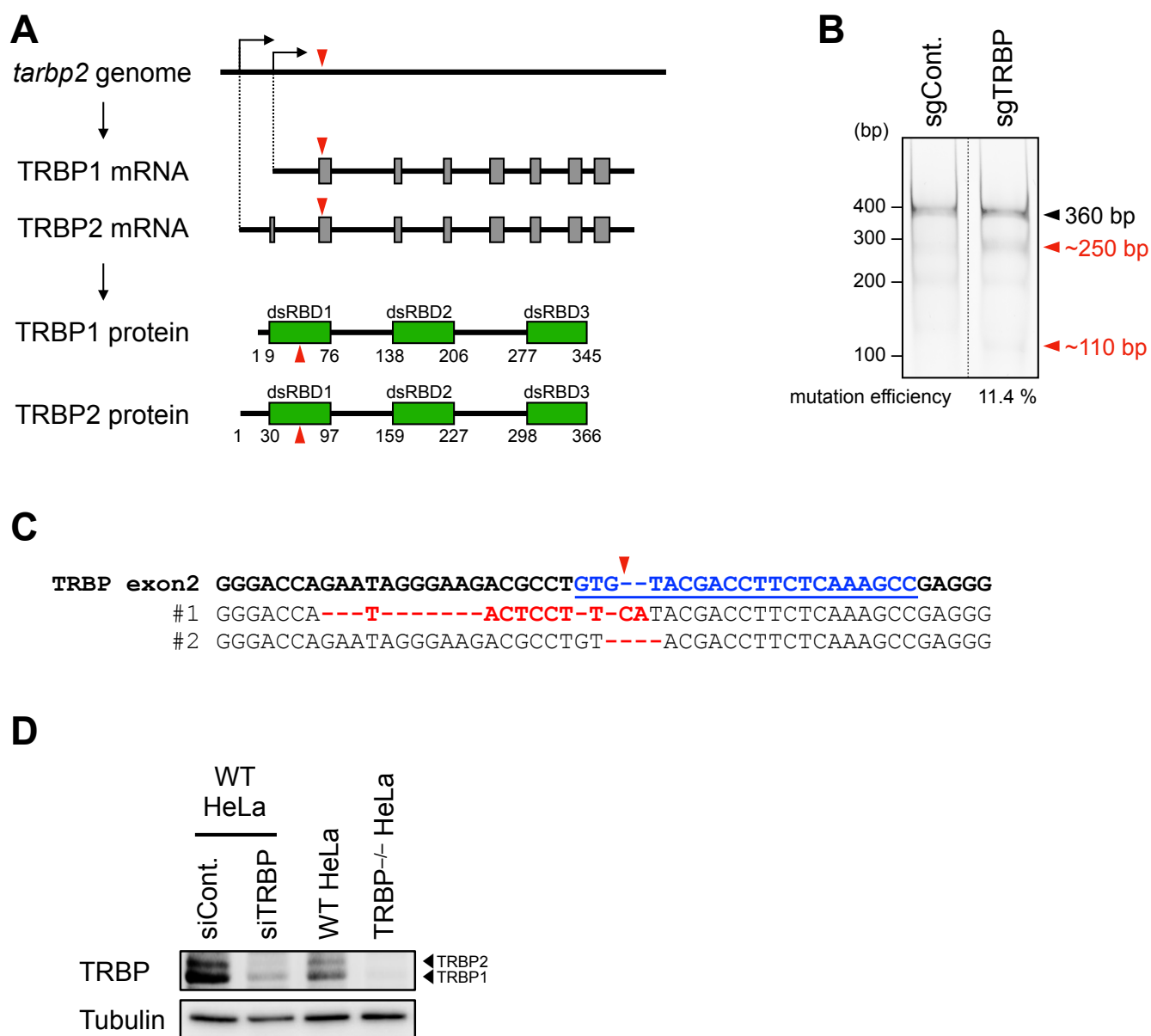
**Figure.5 Immunoprecipitation of RLRs and Dicer using FLAG-TRBP protein in HeLa cells.**

A plasmid encoding N-terminal FLAG-tagged human TRBP (FLAG-TRBP) was transfected into HeLa cells with or without IFN treatment, and immunoprecipitation was performed using anti-FLAG antibody. IgG was used as a negative control. Endogenous RLRs and Dicer were detected by specific antibodies by western blot. TRBP was detected by anti-FLAG antibody. LGP2, but not RIG-I and MDA5, interacted with TRBP.



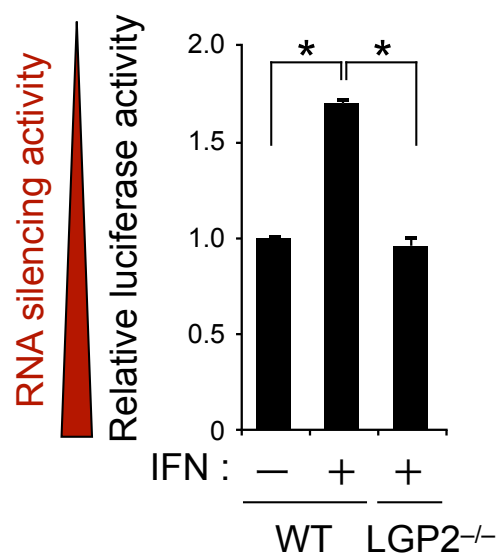
## Figure.6 Establishment of LGP2 knock-out HeLa cells (LGP2<sup>-/-</sup>)

(A) SgRNA was designed against exon 1 of the *lgp2* gene. The gray boxes indicate exons. The arrowheads, the predicted Cas9 cleavage sites. (B) T7EI assay for mutations in the *lgp2* locus induced by CRISPR/Cas9 system. HeLa cells were transfected with plasmids encoding sgLGP2 or sgControl against GFP (sgCont.) and Cas9, and genomic DNA were extracted. The DNA fragment containing the target site of sgLGP2 was amplified by PCR shown in black arrowhead (437 bp). The PCR products were digested with T7EI. Red arrowheads indicate the DNA bands cleaved by T7EI (350 bp and 80 bp). The intensity of bands showed the mutation efficiency of sgLGP2 was 17.4 %. The used primers are shown in Table 2. (C) *lgp2* sequences in cloned LGP2<sup>-/-</sup> cells. Four patterns of mutations were detected. The blue line indicated the complementary region of the sgRNA used. The red indicates the modified region. (D) Western blot was performed using IFN-treated WT and LGP2<sup>-/-</sup> HeLa cells transfected with siControl (siCont.) against GFP or siLGP2.



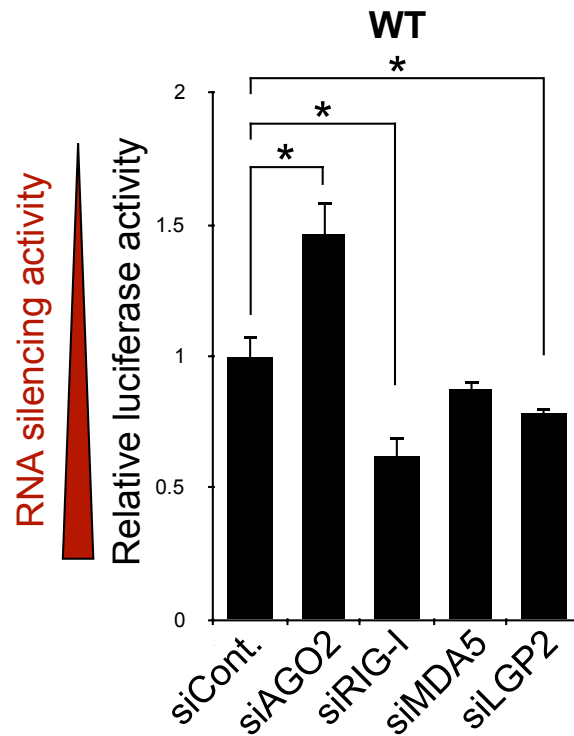
## Figure.7 Establishment of TRBP knock-out HeLa cells (TRBP<sup>-/-</sup>)

(A) sgRNA was designed against exon 2 of the *tarbp2* gene. Exon 2 is a common region of two TRBP transcript variants, TRBP1 and TRBP2. The gray boxes indicate exons. The arrowheads, the predicted Cas9 cleavage sites. (B) T7EI assay for mutations in the *trbp2* locus induced by CRISPR/Cas9 system. HeLa cells were transfected with plasmids encoding sgTRBP or sgCont. and Cas9, and genomic DNA were extracted. The DNA fragment containing the target site of sgTRBP was amplified by PCR shown in black arrowhead (360 bp). The PCR products were digested with T7EI. Red arrowheads indicate the DNA bands cleaved by T7E1 (250 bp and 110 bp). The intensity of bands showed the mutation efficiency of sgTRBP was 11.4 %. The used primers are shown in Table 2. (C) *tarbp2* sequences in cloned TRBP<sup>-/-</sup> cells. Two patterns of mutations were detected. The blue line indicates the complementary region of the sgRNA used. The red indicates the modified region. (D) Western blot was performed using WT and TRBP<sup>-/-</sup> HeLa cells transfected with siCont. against GFP or siTRBP.



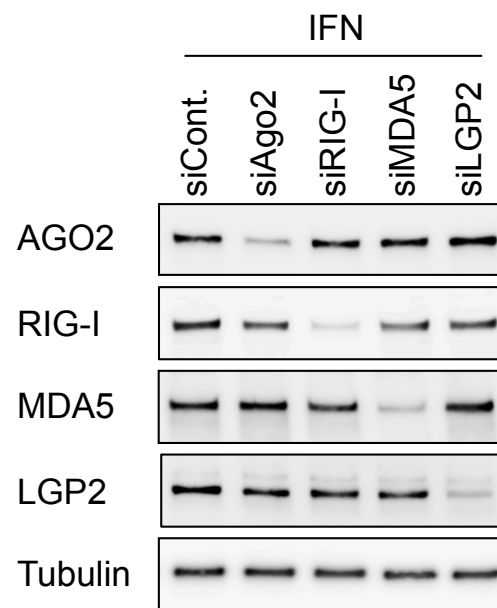
**Figure.8 RNA silencing activity in WT or LGP2<sup>-/-</sup> HeLa cells with or without IFN treatment.**

RNA silencing activity was measured by dual luciferase reporter assay in WT or LGP2<sup>-/-</sup> HeLa cells with or without IFN treatment. Plasmids encoding firefly *luciferase* and pre-miRNA against firefly *luciferase* were transfected into WT or LGP2<sup>-/-</sup> HeLa cells. A plasmid encoding *Renilla luciferase* was co-transfected as an internal control. Relative luciferase activity was calculated by a following formula; firefly luciferase activity / *Renilla luciferase* activity. *P*-values were determined by Student's *t*-test (\**p*<0.05).



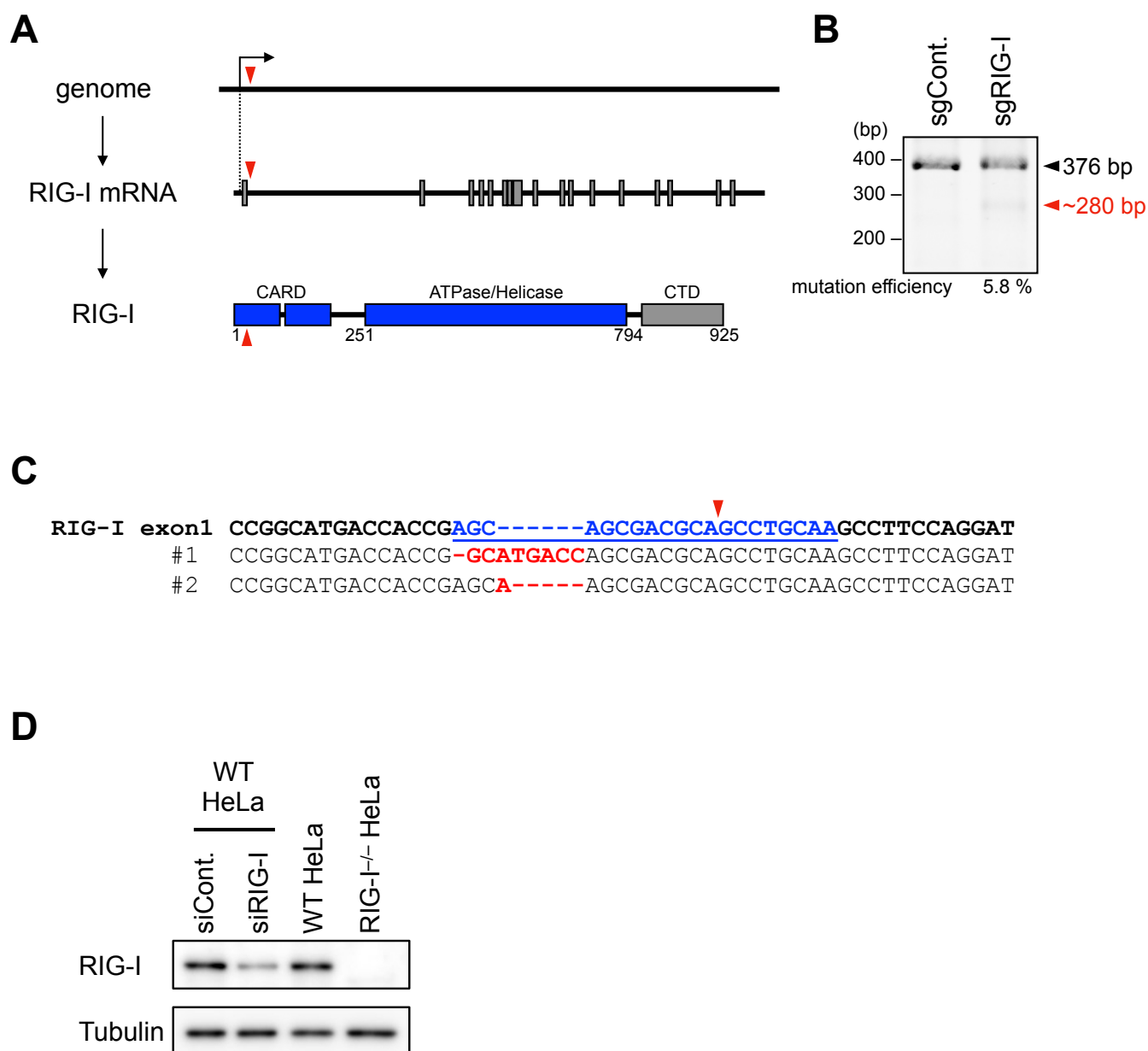
### Figure.9 RNA silencing activity in WT HeLa cells with IFN treatment.

RNA silencing activity was measured by dual luciferase reporter assay in IFN-treated HeLa cells with knockdown of each gene using specific siRNAs. Plasmids encoding firefly *luciferase* and pre-miRNA against firefly *luciferase* were transfected into HeLa cells. A plasmid encoding *Renilla luciferase* was co-transfected as an internal control. Relative luciferase activity was calculated by a following formula; firefly luciferase activity / *Renilla luciferase* activity. This assay was performed by Dr. T. Takahashi. *P*-values were determined by Student's *t*-test (\**p*<0.05).



**Figure.10 Western blots of WT HeLa cells transfected with each specific siRNAs against AGO2, RIG-I, MDA5, or LGP2.**

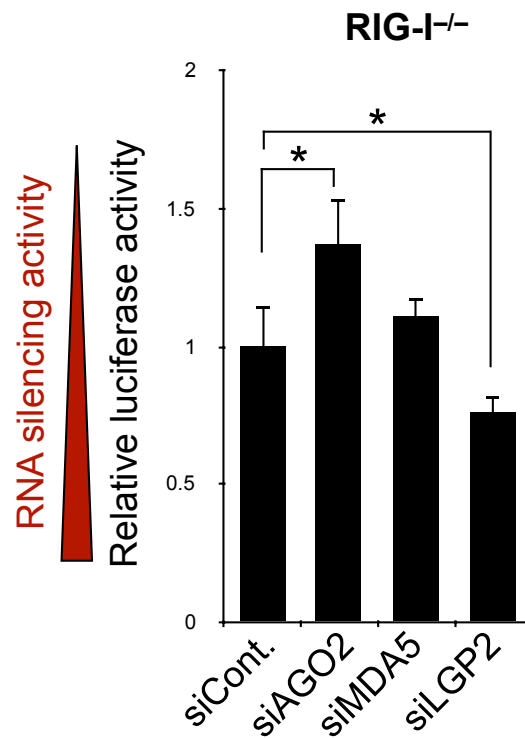
Each specific siRNAs against AGO2, RIG-I, MDA5, or LGP2 was transfected into IFN-treated RIG-I<sup>-/-</sup> HeLa cells. Endogenous AGO2, RIG-I, MDA5, and LGP2 were detected by specific antibodies by western blot. This assay was performed by Dr. T. Takahashi. These protein levels were sufficiently repressed by each siRNA.



## Figure.11 Establishment of RIG-I knock-out HeLa cells (RIG-I<sup>-/-</sup>)

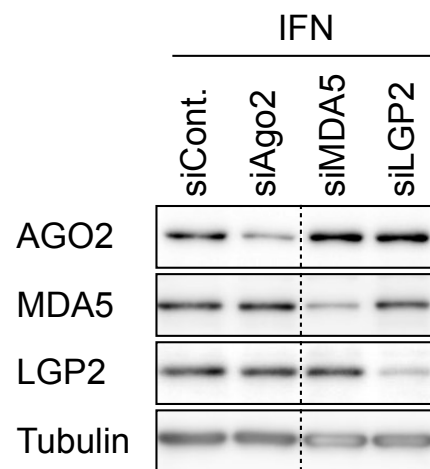
(A) SgRNA was designed against exon 1 of the *rig-I* gene. The gray boxes indicate exons. The arrowheads, the predicted Cas9 cleavage sites. (B) T7EI assay for mutations in the *rig-I* locus induced by CRISPR/Cas9 system. HeLa cells were transfected with plasmids encoding sgRIG-I or sgCont. against GFP and Cas9, and genomic DNA were extracted. The DNA fragment containing the target site of sgRIG-I was amplified by PCR shown in black arrowhead (376 bp). The PCR products were digested with T7EI. Red arrowheads indicate the DNA bands cleaved by T7EI (280 bp). The intensity of bands showed the mutation efficiency of sgRIG-I was 5.8 %. The used primers are shown in Table 2. (C) *rig-I* sequences in cloned RIG-I<sup>-/-</sup> cells. Two patterns of mutations were detected. The blue line indicates the complementary region of the sgRNA used. The red indicates the modified region. (D) Western blot was performed using IFN-treated WT and RIG-I<sup>-/-</sup> HeLa cells transfected with siCont. against GFP or siRIG-I.





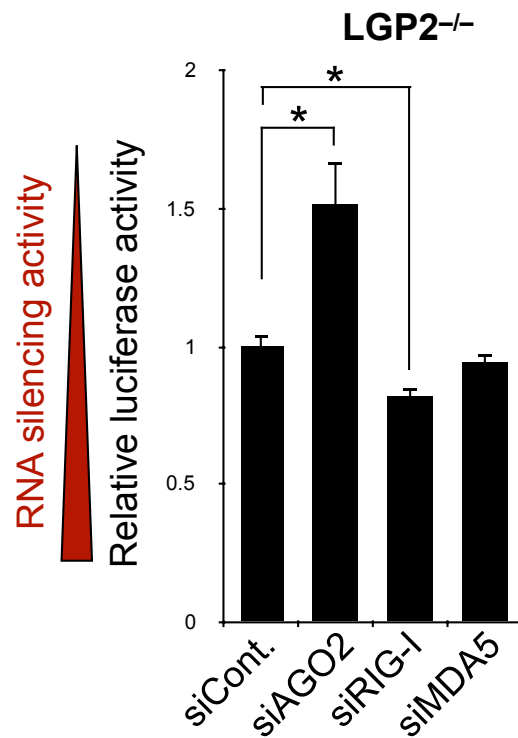
### Figure.12 RNA silencing activity in RIG-I<sup>-/-</sup> HeLa cells with IFN treatment.

RNA silencing activity was measured by dual luciferase reporter assay in IFN-treated RIG-I<sup>-/-</sup> HeLa cells with knockdown of each gene using specific siRNAs. Plasmids encoding pre-miRNA against firefly *luciferase*, firefly *luciferase*, and *Renilla luciferase* were transfected into RIG-I<sup>-/-</sup> HeLa cells simultaneously. *P*-values were determined by Student's *t*-test (\**p*<0.05).



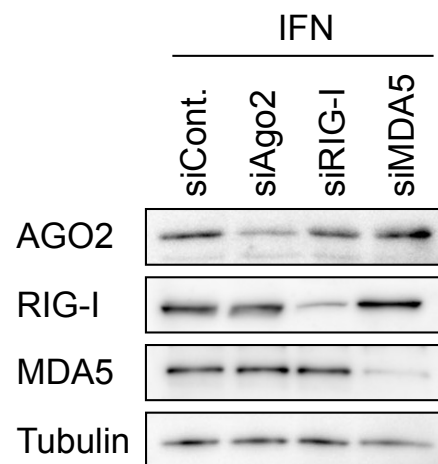
**Figure.13 Western blots of RIG-I<sup>-/-</sup> HeLa cells transfected with each specific siRNAs against AGO2, MDA5, or LGP2.**

Each specific siRNAs against AGO2, MDA5, or LGP2 was transfected into IFN-treated RIG-I<sup>-/-</sup> HeLa cells. Endogenous AGO2, MDA5, and LGP2 were detected by specific antibodies by western blot. These protein levels were sufficiently repressed by each siRNA.



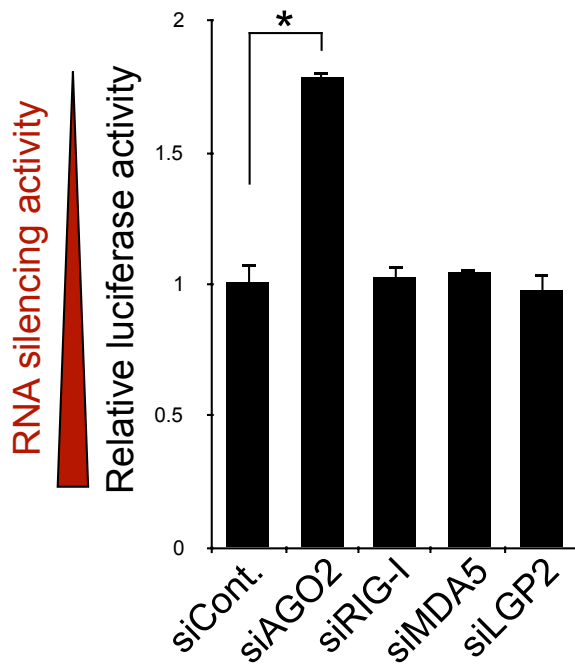
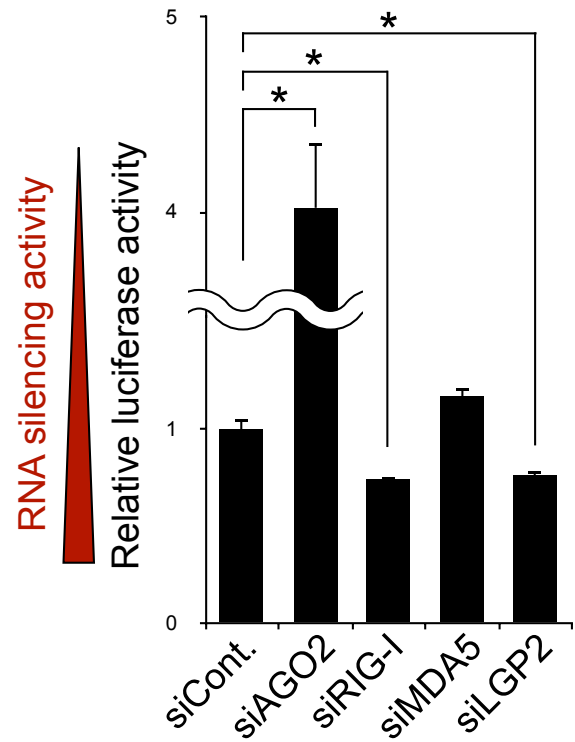
**Figure.14 RNA silencing activity in LGP2<sup>-/-</sup> HeLa cells with IFN treatment.**

RNA silencing activity was measured by dual luciferase reporter assay in IFN-treated LGP2<sup>-/-</sup> HeLa cells with knockdown of each gene using specific siRNAs. Plasmids encoding pre-miRNA against firefly *luciferase*, firefly *luciferase*, and *Renilla luciferase* were transfected into LGP2<sup>-/-</sup> HeLa cells simultaneously. *P*-values were determined by Student's *t*-test (\**p*<0.05).



**Figure.15 Western blots of LGP2<sup>-/-</sup> HeLa cells transfected with each specific siRNAs against AGO2, RIG-I, or LGP2.**

Each specific siRNAs against AGO2, RIG-I, or MDA5 was transfected into IFN-treated LGP2<sup>-/-</sup> HeLa cells. Endogenous AGO2, RIG-I, and MDA5 were detected by specific antibodies by western blot. These protein levels were sufficiently repressed by each siRNA.

**A****B**

### Figure.16 RNA silencing activity in TRBP<sup>-/-</sup> HeLa cells with IFN treatment.

(A) RNA silencing activity was measured by dual luciferase reporter assay in IFN-treated TRBP<sup>-/-</sup> HeLa cells with knockdown of each gene using specific siRNAs. Plasmids encoding pre-miRNA against firefly luciferase, firefly luciferase, and *Renilla luciferase* were transfected into TRBP<sup>-/-</sup> HeLa cells simultaneously. (B) A plasmid encoding TRBP was transfected into TRBP<sup>-/-</sup> HeLa cells. RNA silencing activity was measured by dual luciferase reporter assay. Plasmids encoding pre-miRNA against firefly luciferase, irefly luciferase, and *Renilla luciferase* were transfected into TRBP<sup>-/-</sup> HeLa cells with knockdown of each gene using specific miRNAs. *P*-values were determined by Student's *t*-test (\**p*<0.05).

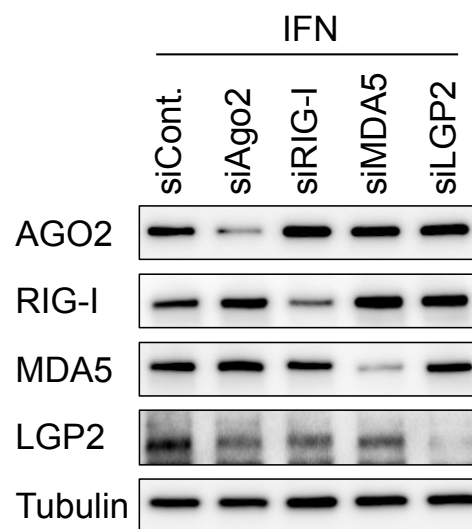


**Figure.17 Western blots of TRBP<sup>-/-</sup> HeLa cells transfected with each specific siRNAs against AGO2 and RLRs, respectively.**

Each specific siRNAs against AGO2 and RLRs was transfected into IFN-treated TRBP<sup>-/-</sup> HeLa cells, respectively. Endogenous AGO2 and RLRs were detected by specific antibodies by western blot. These protein levels were sufficiently repressed by each siRNA.

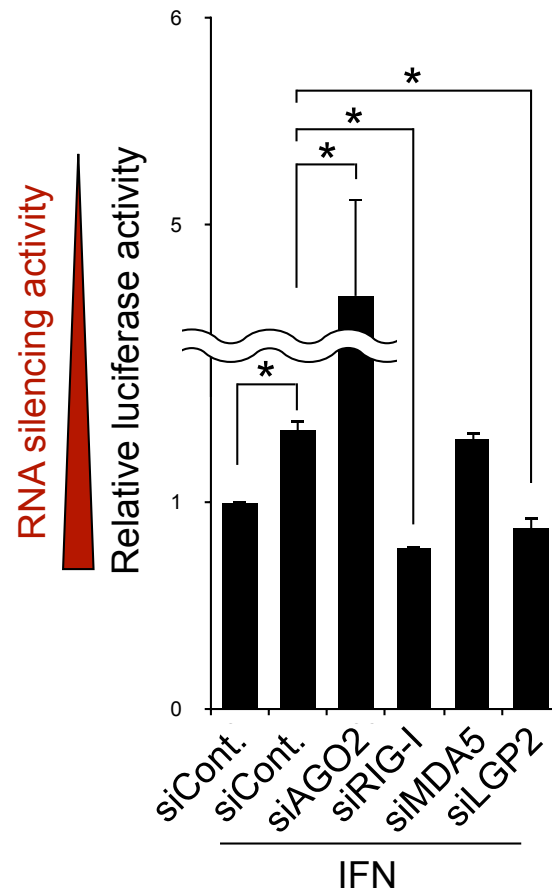


### Figure.18 LGP2 and RIG-I represses RNA silencing activity in HEK293 cells

RNA silencing activity was measured by dual luciferase reporter assay in HEK293 cells with knockdown of AGO2, RIG-I, MDA5, or LGP2 using specific siRNAs. siRNA against GFP was used as a control. Plasmids encoding pre-miRNA against firefly *luciferase*, firefly *luciferase*, and *Renilla luciferase* were transfected into IFN-treated HEK293 cells simultaneously. *P*-values were determined by Student's *t*-test (\**P*<0.05).

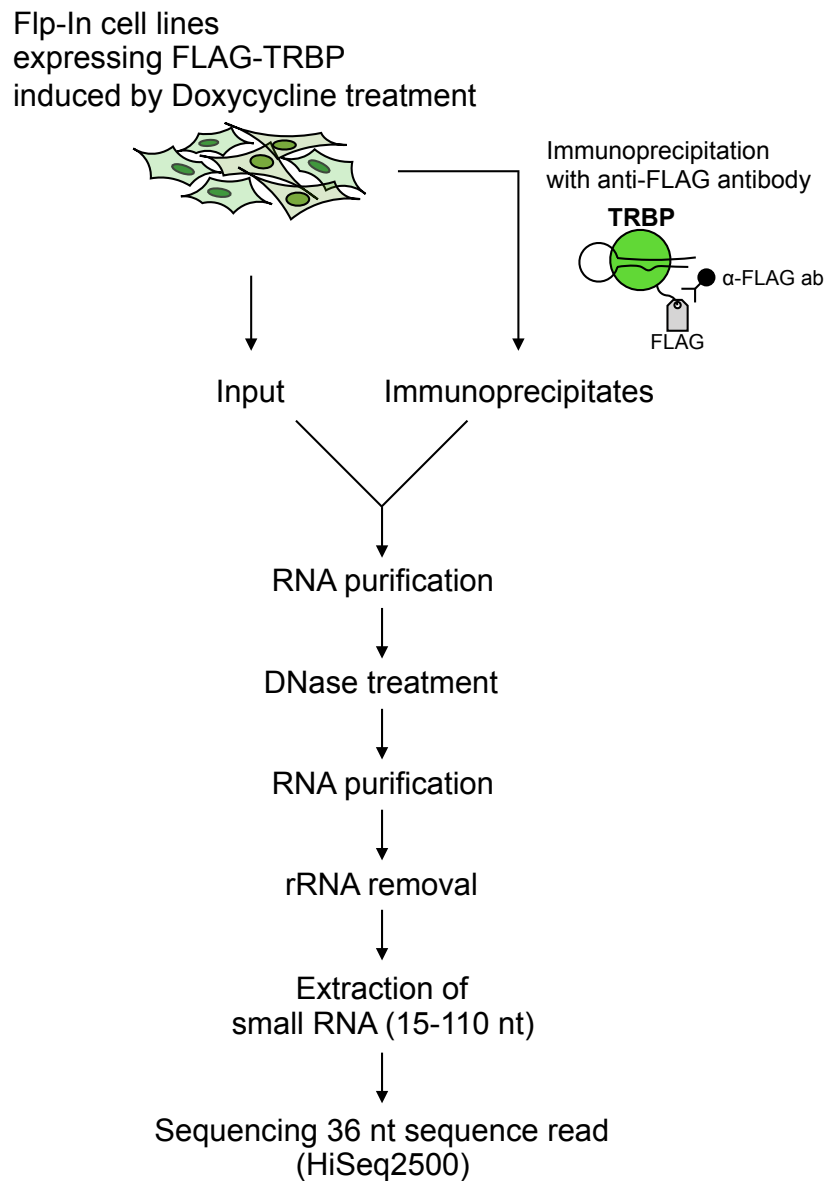


### Figure.19 Procedure for RIP-sequencing

Procedure for RIP-seq. Flp-In 293 FLAG-TRBP cells were treated with Doxycycline and the expression of FLAG-TRBP was induced. TRBP-bound RNAs were collected by immunoprecipitation with anti-FLAG antibody. DNA and rRNA were removed by DNase treatment and RiboZero treatment, respectively. Small RNAs were extracted and sequenced by HiSeq2500.



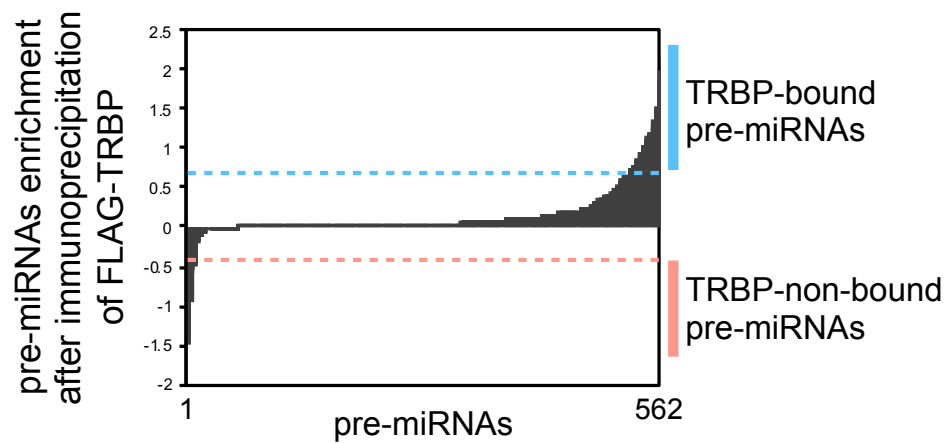
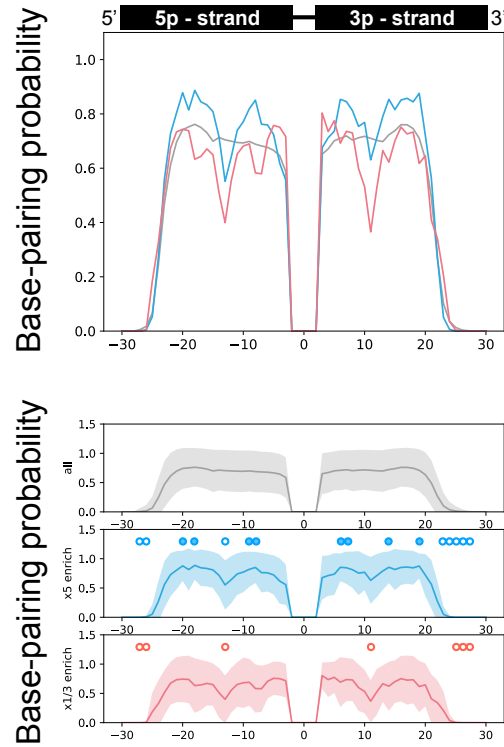


**Figure.20 Enrichment analysis of TRBP-bound pre-miRNAs.**

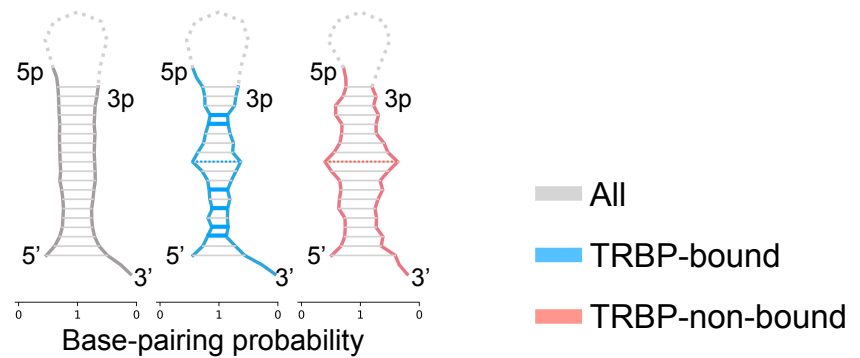
Enrichment of sequence read of RIP-seq by immunoprecipitation was calculated with input RNA not subjected to immunoprecipitation (immunoprecipitation / input). 562 pre-miRNAs were immunoprecipitated with TRBP. Top 40 pre-miRNAs (enrichment > 5) were defined as TRBP-bound pre-miRNAs shown in blue. Bottom 10 pre-miRNAs (enrichment < 1/3) were defined as TRBP-non-bound pre-miRNAs shown in pink.

**A**



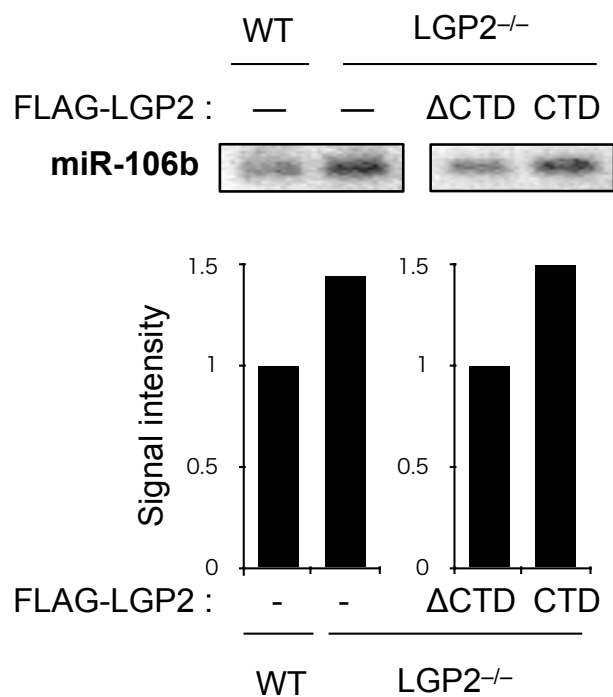
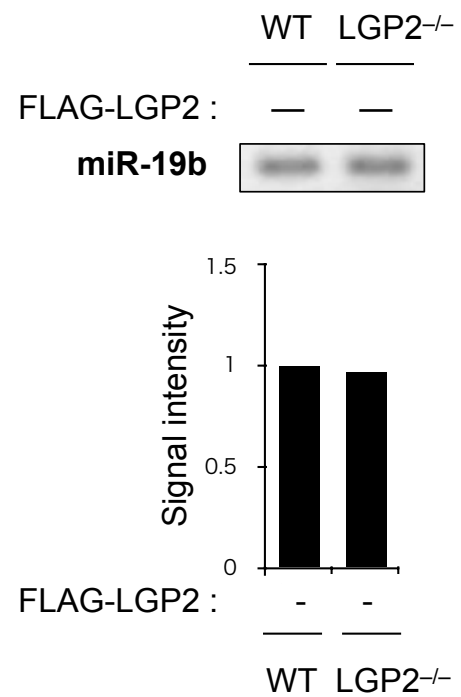
**B**

Predicted secondary structure of pre-miRNAs



## Figure.21 Predicted secondary structure of TRBP-bound pre-miRNAs.

(A) In upper panel, bpp values of 40 TRBP-bound pre-miRNAs (blue), 10 TRBP-non-bound pre-miRNAs (pink), and all 1761 pre-miRNAs registered in miRBase (gray) were calculated using CentroidFold. Positions of 5p and 3p miRNA are shown -30~-3 and 3~30 on X-axis, respectively. Vertical axis indicates bpps at each location. In lower panel, solid lines indicate mean values of bpps. Colored regions indicate standard deviations.  $P$ -values were determined by Student's  $t$ -test ( $*p<0.05$ ). Filled circle and open circle indicate significantly higher bpps and significantly lower bpps compared to control, respectively. (B) Schematic diagrams of predicted secondary structures of stem regions of TRBP-bound pre-miRNAs, TRBP-non-bound pre-miRNAs, and all pre-miRNAs in the stem region. Colored solid lines and dashed lines indicate significantly higher and lower bpp, respectively. TRBP-bound pre-miRNAs showed tighter base-pairing in the stem region compared to control.

**A****B**

### Figure.22 Mature miRNA levels of TRBP-bound miR-106b and TRBP-non-bound miR-19b in WT and LGP2<sup>-/-</sup> HeLa cells.

(A) A plasmid encoding N-terminal FLAG-tagged LGP2-ΔCTD or -CTD was transfected into LGP2<sup>-/-</sup> HeLa cells. Mature miRNA levels of TRBP-bound miR-106b in WT and LGP2<sup>-/-</sup> HeLa cells were detected by RT-PCR and quantified by the signal intensities. (B) Mature miRNA levels of TRBP-non-bound miR-19b in WT and LGP2<sup>-/-</sup> HeLa cells were detected by RT-PCR. Signal intensities were measured in the lower panels. LGP2 decreased TRBP-bound miR-106b via helicase domain, since the expression of LGP2-ΔCTD, mainly containing helices domain, decreased the amount of mature miR-106b.

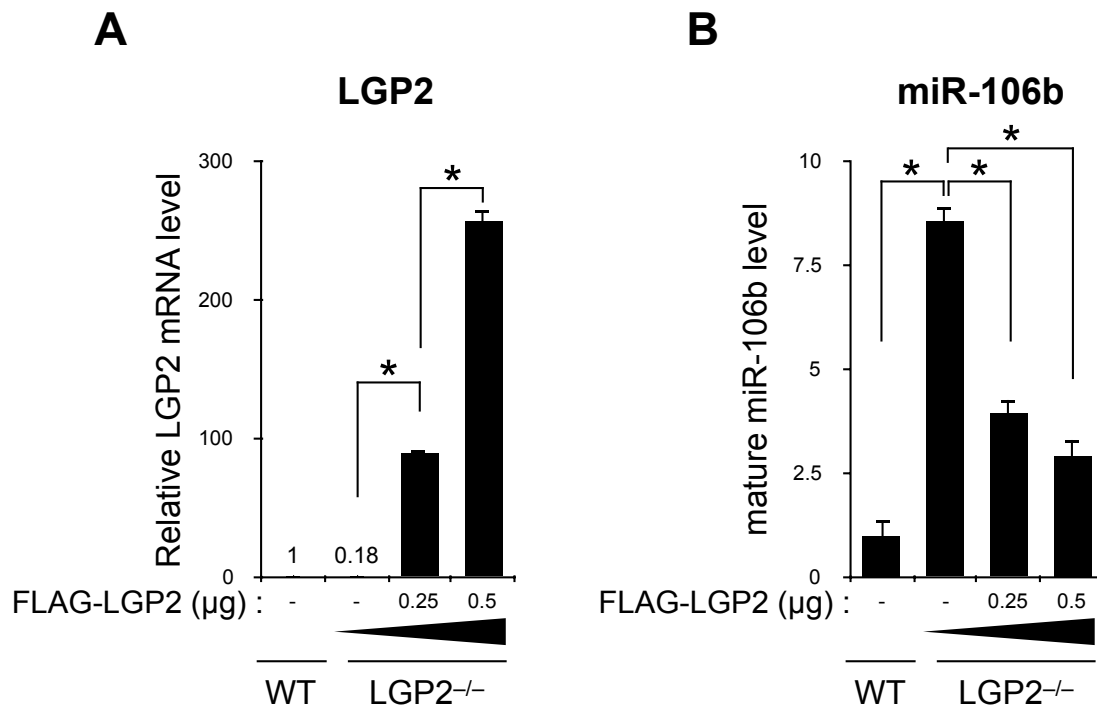


**Figure.23 Mature miRNA levels of TRBP-bound miR-106b in WT and LGP2<sup>-/-</sup> HeLa cells.**

(A) A plasmid encoding N-terminal FLAG-tagged LGP2 was transfected into LGP2<sup>-/-</sup> HeLa cells at three different concentration (0, 0.25, 0.5 μg). LGP2 mRNA levels were measured by qRT-PCR and normalized by Tubulin. (B) TRBP-bound miR-106b levels in WT and LGP2<sup>-/-</sup> HeLa cells were measured by qRT-PCR. *P*-values were determined by Student's *t*-test (\**p*<0.05).

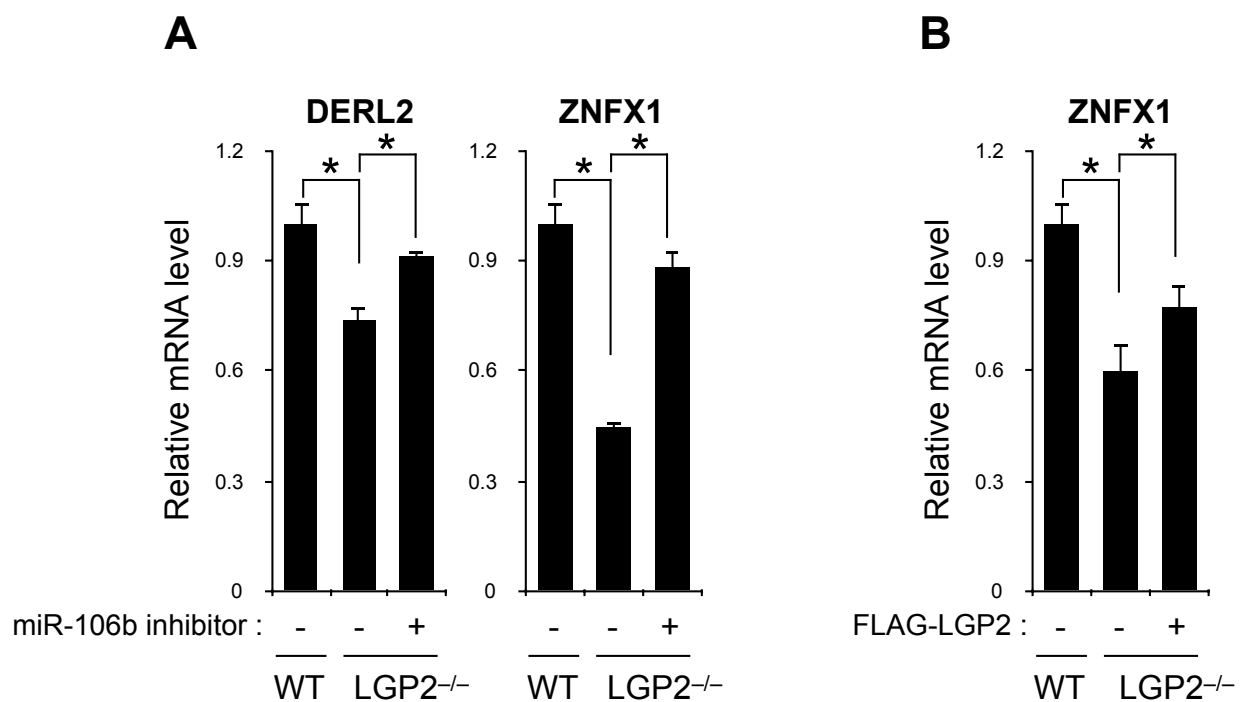


**Figure.24 mRNA levels of target genes of TRBP-bound miR-106b in WT and LGP2<sup>-/-</sup> HeLa cells.**

(A) A plasmid encoding miR-106b inhibitor (TuD-miR-106b) or TuD-shuttle as a control was transfected into WT or LGP2<sup>-/-</sup> HeLa cells, and mRNA levels of TRBP-bound miR-106b targets, DERL2 and ZNFX1, were measured by qRT-PCR. (B) A plasmid encoding N-terminal FLAG-tagged LGP2 was transfected into LGP2<sup>-/-</sup> HeLa cells and mRNA level of ZNFX1 was measured by qRT-PCR in WT and LGP2<sup>-/-</sup> HeLa cells. Relative target mRNA levels were normalized by Tubulin mRNA level. *P*-values were determined by Student's *t*-test (\**p*<0.05). LGP2 upregulated target genes of TRBP-bound miR-106b.

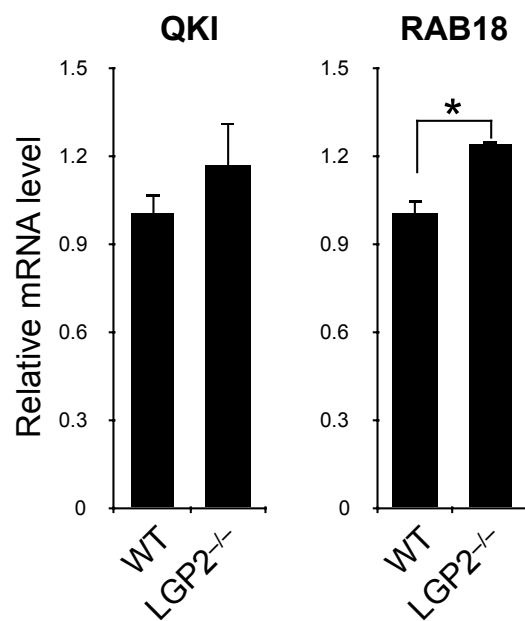


**Figure.25 mRNA levels of target genes of TRBP-non-bound miR-19b in WT and LGP2<sup>-/-</sup> HeLa cells.**

mRNA levels of TRBP-non-bound miR-19b targets, QKI and RAB18, were measured by qRT-PCR in WT and LGP2<sup>-/-</sup> HeLa cells. Relative target mRNA levels were normalized by Tubulin mRNA level. *P*-values were determined by Student's *t*-test (\**p*<0.05). Target genes of TRBP-non-bound miR-19b were not decreased by LGP2 knock-out.

**Table.1 Oligonucleotides used for knockdown**

siRNA name	Guide strand sequence (5' -> 3')	Passenger strand sequence (5' -> 3')
siControl	AUGAUAUAGACGUUGUGGCUG	GCCACAACGUCUAUAUCAUGG
siAGO2	AAUCUCUUCUUGCCGAUCGGG	CGAUCGGCAAGAAGAGAUUAG
siRIG-I	UAAAUUCUGGUUGUAAACGUU	CGUUUACAACCAGAAUUUAAA
siMDA5	AGUAAAUGCAUCAAGAUUGGC	CAAUCUUGAUGCAUUUACUAI
siLGP2	UCAUGAUGACGUUGUAGACGG	GUCUACAACGUCAUCAUGAGC
siIPS-1	UCGUCCGCGAGAUCAACUAdTdT	UAGUUGAUCUCGCGGACGAdTdT

**Table.2 Oligonucleotides used for generation of knock-out HeLa cells**

name	sequence (5' -> 3')
TRBP sgRNA sense	GATCCCGCTTTGAGAAGGTCGTACAC
TRBP sgRNA antisense	AAACGTGTACGACCTTCTCAAAGCGG
TRBP-F	GGGCCCTACTTTTCCAGCCTG
TRBP-R	CAAGCCTTCCTCACCAGTGCA
LGP2 sgRNA sense	GATCCCGGGCTGCTTATGTGGCCAAG
LGP2 sgRNA antisense	AAACCTTGGCCACATAAGCAGCCCGG
LGP2-F	GGCAGACCTACCTACTAGAGCAG
LGP2-R	TGAACTCTTCACCATGCTGG
RIG-I sgRNA sense	GATCCCGTGCAGGCTGCGTCGCTGCT
RIG-I sgRNA antisense	AAACAGCAGCGACGCAGCCTGCACGG
RIG-I-F	AATCCCTGCTTTCCCCGCTC
RIG-I-R	GGGCTCCTCAAACCTCTGGCA

F indicates forward primer. R indicates reverse primer.



**Table.3 Oligonucleotides used for the construction  
of a plasmid expressing TuD-miR-106b**

name	sequence (5' -> 3')
TuDmiR-106b sense	CATCAACATCTGCACTGTGGACCAGCACTTTACAAGTATTCTGGTCACAGAATACAA CATCTGCACTGTGGACCAGCACTTTACAAG
TuD-miR-106b antisense	TCATCTTGTAAGTGCTGGTCCACAGTGCAGATGTTGTATTCTGTGACCAG AATACTTGTAAGTGCTGGTCCACAGTGCAGATGTT

**Table.4 Oligonucleotides used for RT-PCR**

name	sequence (5' -> 3')
hTubulinB-F	CTGGCACCATGGACTCTG
hTubulinB-R	TCGGCTCCCTCTGTGTAG
hIFN-B-F	AAACTCATGAGCAGTCTGCA
hIFN-B-R	AGGAGATCTTCAGTTTCGGAGG
hOAS1-F	TTGATGCCCTGGGTCAGTTG
hOAS1-R	AGAACTCGCCCTCTTTCTGC
hOAS2-F	CAGAAGCCCAGGCCTATCATC
hOAS2-R	ATGCCATTCCGTCCCATGC
hOAS3-F	CAGAAGCCCAGGCCTATCATC
hOAS3-R	ATGCCATTCCGTCCCATGC
hIPS-1-F	ATAAGTCCGAGGGCACCTTT
hIPS-1-R	GTGACTACCAGCACCCCTGT
hDERL2-F	TATGTGTGGAGCCGAAGGAACC
hDERL2-R	TGCAATACCCAAAAGGTCCACAATG
hZNFX1-F	TGGACCAGTGCAGGATAGTGAA
hZNFX1-R	TGCGTGAAAGAACCGACACC
hQKI-F	TCCTCACCCAACTGCTGCAA
hQKI-R	AGCCACCGCACCTAATACAC
hRAB18-F	AGGATGGACGAGGACGTGCTAA
hRAB18-R	TGAACCTCAAGAGCAGGCTGGA
miR-106b-5p-RT	GTCGTATCCAGTCAGGGTCCGAGGTATTCGCACTGGATACGACATCTGC
miR-106b-5p-F	GCCGCTAAAGTGCTGACAGT
miR-106b-5p-R	GTGCAGGGTCCGAGGT
miR-19b-3p-RT	GTCGTATCCAGTGCAGGGTCCGAGGTATTCGCACTGGATACGACTCAGTT
miR-19b-3p-F	GCCGCTGTGCAAATCCATGCAA
miR-19b-3p-R	GTGCAGGGTCCGAGGT

F indicates forward primer. R indicates reverse primer. RT, reverse transcription primer

**Table.5 TRBP-bound 40 pre-miRNAs  
(Enrichment > 5)**

	pre-miRNA_name	enrichment
1	hsa-mir-708	143.19
2	hsa-mir-31	95.41
3	hsa-mir-25	71.12
4	hsa-mir-140	69.91
5	hsa-mir-582	35.80
6	hsa-mir-340	32.76
7	hsa-mir-30a	30.98
8	hsa-mir-1226	28.59
9	hsa-mir-7641-2	26.70
10	hsa-mir-590	22.16
11	hsa-mir-16-1	21.74
12	hsa-mir-503	19.05
13	hsa-mir-10b	17.04
14	hsa-mir-766	16.28
15	hsa-let-7a-3	16.20
16	hsa-mir-378a	15.39
17	hsa-mir-106b	14.49
18	hsa-mir-500a	13.63
19	hsa-mir-6087	12.98
20	hsa-mir-345	11.59
21	hsa-mir-605	10.97
22	hsa-mir-33b	10.36
23	hsa-mir-196a-1	9.65
24	hsa-mir-181b-1	9.60
25	hsa-mir-1304	9.06
26	hsa-mir-636	8.89
27	hsa-mir-324	7.90
28	hsa-mir-30e	7.62
29	hsa-mir-126	7.26
30	hsa-mir-29c	7.22
31	hsa-mir-181d	6.56
32	hsa-mir-2278	6.56
33	hsa-mir-101-1	6.31
34	hsa-mir-1292	6.13
35	hsa-mir-30b	5.99
36	hsa-mir-181a-1	5.83
37	hsa-mir-196a-2	5.60
38	hsa-mir-3928	5.52
39	hsa-mir-218-1	5.31
40	hsa-mir-744	5.21

**Table.6 TRBP-non-bound 10 pre-miRNAs  
(Enrichment > 1/3)**

	pre-miRNA_name	enrichment
553	hsa-mir-33a	0.33
554	hsa-mir-3651	0.32
555	hsa-mir-374a	0.30
556	hsa-mir-23a	0.28
557	hsa-mir-15a	0.25
558	hsa-mir-1291	0.11
559	hsa-mir-20a	0.09
560	hsa-mir-19b-1	0.06
561	hsa-mir-3653	0.04
562	hsa-mir-3607	0.03